

THESIS FOR THE DEGREE OF LICENTIATE OF ENGINEERING

NO_x Formation in Rotary Kilns for Iron Ore Pelletization

Rikard Edland

Department of Space, Earth and Environment

CHALMERS UNIVERSITY OF TECHNOLOGY

Gothenburg, Sweden 2017

NO_x Formation in Rotary Kilns for Iron Ore Pelletization

RIKARD EDLAND

© RIKARD EDLAND, 2017.

Department of Space, Earth and Environment
Chalmers University of Technology
SE-412 96 Gothenburg
Sweden
Telephone + 46 (0)31-772 1000

Printed by Chalmers Reproservice
Chalmers University of Technology
Gothenburg, Sweden 2017

RIKARD EDLAND

Division of Energy Technology
Department of Space, Earth and Environment
Chalmers University of Technology

Abstract

The production of iron ore pellets is often performed in the so-called Grate-Kiln process. The aim of the process is to oxidize the magnetite (Fe₃O₄) to hematite (Fe₂O₃) and to sinter the pellets so they can be used in steel manufacturing. The heat required for this is produced by combusting a pulverized fuel in a rotary kiln, forming a suspension flame. Due to the need to oxidize the pellets, large amounts of air are introduced to the kiln. Relating the amount of air to the fuel, an air-to-fuel equivalence ratio of 4-6 is obtained. Furthermore, the air is pre-heated to above 1000°C. High temperatures and large amounts of excess air are known to promote NO_x formation and NO_x emissions from iron ore processing plants are in general high.

The aim of this work is to describe the NO formation in the rotary kiln and to identify governing parameters that may be altered to reduce the emissions. The thesis contains results from experiments in a pilot-scale kiln and from modeling work based on the same experiments. In the experiments, four coals were tested as well as co-firing coal with biomass. In-flame measurements of temperature and gas concentrations were performed with the use of a suction pyrometer and FTIR spectroscopy (+paramagnetism). Different primary measures for NO_x reduction were also tested. Overall, reducing the primary air flow in the burner and co-firing coal with biomass were the most effective measures for reducing NO_x emissions, compared to the reference case. Using natural gas and oil resulted in three times the amount of NO_x. Reducing the total amount of excess air only resulted in a small NO_x reduction, and increasing the secondary air temperature resulted in slightly decreased NO_x formation.

The general assumption in rotary kilns is that NO_x is mostly formed by the thermal NO mechanism due to the high temperatures involved. Although this is certainly true for the cases with gas and oil, the experimental results indicate that NO_x formed from the fuel-bound nitrogen is dominating the total NO_x formation when solid fuels are used. The results from the detailed reaction modeling show that the thermal NO formation is of minor importance. Instead, the reduction of NO by char appears to be remarkably low in the kiln and responsible for the high net conversion of fuel-bound nitrogen to NO.

Keywords: Nitrogen oxides, combustion chemistry, NO_x formation, emissions control, rotary kiln, Grate-Kiln process

List of Publications

This thesis is based on the following papers:

- I. R. Edland, F. Normann, C. Fredriksson, K. Andersson, *Implications of Fuel Choice and Burner Settings for Combustion Efficiency and NO_x Formation in PF-Fired Iron Ore Rotary Kilns*, *Energy and Fuels*, 2017, 31 (3), pp 3253–3261
- II. R. Edland, F. Normann, K. Andersson, *Modelling the contribution from volatile and char bound nitrogen to NO_x formation in iron ore rotary kilns*, Submitted for publication, 2017
- III. R. Edland, F. Normann, K. Andersson, *Nitrogen chemistry in rotary kiln flames: Impact of mixing rate and temperature at high air to fuel ratios*, Nordic Flame Days Conference 2016

Rikard Edland is the main author of all three papers. Associate Professor Fredrik Normann and Professor Klas Andersson contributed with guidance for the modeling and experimental work, as well as to the editing of the papers. Dr. Christian Fredriksson was responsible for the planning and evaluation of the experimental campaign at LKAB (Paper I).

Acknowledgments

I would like to start off by expressing my gratitude to my supervisors Professor Klas Andersson and Associate Professor Fredrik Normann for all your guidance and willingness to share your expertise, as well as helping me develop as a researcher and teacher. I would also like to thank my examiner Professor Filip Johnsson for providing valuable input to this thesis. The Swedish Energy Agency and LKAB are acknowledged for their financial support of this work. An extra appreciation goes to Christian Fredriksson at LKAB for fruitful discussions and for planning the experimental campaign that much of this thesis is based on.

A special thanks to Adrian Gunnarsson for your enjoyable company, efficient cooperation and solid support during our work together. Thomas Ekvall receives my appreciation for teaching me about our experimental facility, as well as always being willing to discuss combustion chemistry and video games. Daniel Bäckström is also greatly appreciated for all the help with many experiments, and for taking care of that unruly FTIR.

To the rest of the Combustion and Carbon Capture Technologies group and everyone else at Energy Technology: Thank you for being who you are and for contributing to a stimulating working environment! A special thanks to my officemate Angelica Corcoran for your support and for putting up with my disorderliness.

Thanks to all my friends for making my life (both inside and outside of the Chalmers walls) so active and enjoyable. Thanks to my brother for being a role model and a great friend, and to my father for always believing in me and for thinking that I can fix any technical problem. Last but definitely not least, thanks to my mother who has encouraged me my entire life and with whom I can discuss anything. I wouldn't have made it here without your support.

Rikard Edland
Gothenburg, Sweden
September, 2017

Table of contents

1	Introduction	1
1.1	Aim and scope	1
1.2	Outline of the thesis	1
2	Background.....	3
2.1	Nitrogen oxides	3
2.2	NO _x legislation	3
2.3	Iron ore production	6
3	Theory.....	9
3.1	NO formation routes.....	9
3.2	Fuel-N evolution during solid fuel combustion.....	11
3.3	General NO _x mitigation strategies.....	16
3.4	Units of emission measurements	18
4	Previous work on NO _x in rotary kilns	21
4.1	Cement industry.....	21
4.2	Iron ore industry	22
5	Experimental equipment.....	25
5.1	Experimental Combustion Facility.....	25
5.2	In-flame measurements	26
6	Modeling.....	31
6.1	Overall modelling considerations.....	31
6.2	Model description.....	31
7	Results and discussion.....	35
7.1	NO _x performance.....	35
7.2	Contributions of thermal NO and fuel NO formation mechanisms	37
8	Summary.....	43
9	Future work	45
	References	47

1 Introduction

The production of iron ore pellets, which is vital to the production of steel, is expected to be an important industry for many years to come. The pelletizing of iron ore is often performed in the ‘Grate-Kiln’ process, in which the iron ore is heated, first on a traveling grate and then in a rotary kiln. The pelletizing process is energy-intensive and powered by combustion in the presence of large volumes of hot air ($>1000^{\circ}\text{C}$), usually employing fossil fuels. NO_x emissions from this combustion process are generally high, and these emissions will need to be controlled in order to comply with upcoming NO_x legislation.

In Europe, NO_x emissions have decreased significantly over the last few decades thanks to strict NO_x regulations combined with the development of NO_x mitigation technologies. However, specific features of the Grate-Kiln process, e.g., the rotation of the kiln and the large volumetric gas flows, make conventional methods for NO_x mitigation unfeasible. Therefore, it is important to understand and describe accurately the mechanisms governing NO_x formation in order to identify and evaluate the mitigation possibilities. Recent targets set by the European Parliament to reduce emissions is a major motivating factor for this research.

1.1 Aim and scope

The overall aim of the work is to describe the NO_x formation under combustion conditions that are relevant for the Grate-Kiln process. An important part is to identify governing parameters that are feasible to alter within the constraints of the pelletizing process in order to reduce the NO_x emissions. The NO_x chemistry is evaluated through a combination of pilot-scale experiments and combustion modeling.

1.2 Outline of the thesis

This thesis consists of a summary of the work and the three appended papers. Chapter 2 provides the background related to the effects of NO_x and current legislative measures, as well as a description of the Grate-Kiln process. The aim of this chapter is to set the thesis in an appropriate context. Chapter 3 presents the theoretical framework of the chemistry and the processes that govern NO_x formation. Chapter 4 summarizes the previous research on NO_x mitigation in rotary kilns. Chapters 5 and 6 describe the experimental and numerical methods used. Chapter 7 provides the results and a discussion. The thesis concludes with a summary and ideas for future work.

Paper I is an experimental investigation of the impacts of fuel and combustion parameters on NO_x formation in rotary kilns. Different coals, as well as co-firing of coal and biomass were tested. In-flame measurements of temperature and gas composition were performed with suction pyrometry and FTIR spectroscopy. Paper II evaluates the importance of the NO_x formation mechanisms in iron ore rotary kilns using detailed reaction modeling. Paper III is an investigation of the gas-phase chemistry and how it depends on the combustion temperature and mixing of the fuel and air.

2 Background

2.1 Nitrogen oxides

A nitrogen oxide molecule is composed of nitrogen and oxygen atoms. There are several theoretical possibilities for the arrangement of these atoms, although the only relevant compounds in terms of atmospheric pollution are nitric oxide (NO), nitrogen dioxide (NO₂), and nitrous oxide (N₂O). The term “NO_x” is a generic term for NO and NO₂ (as they are closely related), whereas N₂O is not usually included in this term. N₂O is a potent greenhouse gas (more potent by orders of magnitude than CO₂), although it is not directly hazardous to humans or the environment. In contrast, both NO and NO₂ are inherently toxic and may cause lung injury in humans. NO is considered to be less toxic but is the main precursor of NO₂ and is, therefore, of equal importance. The main problems associated with NO_x are however secondary effects, which result in the formation of tropospheric ozone and acid deposition. Tropospheric ozone (O₃) represents ozone that is close to the ground (the troposphere). Although the ozone in the upper atmosphere (the stratosphere) is important for protecting the planet from UV-radiation, it is hazardous to humans as it harms the respiratory system and causes damage to vegetation and crops [1-3]. Ozone is responsible for many of the negative health effects associated with “smog”, which blights many urban areas around the world. Ozone may be formed by the reaction between an oxygen molecule (O₂) and an oxygen radical (O). While natural concentrations of oxygen radicals are low, the decomposition of NO₂ by sunlight increases this concentration, thereby increasing the level of ozone. The formation of ozone through NO₂ is described by reactions R 2-1 and R 2-2 below, where $h\nu$ is the energy from solar radiation.



The other major problem with NO_x is acid deposition, in the form of either acid rain (wet deposition) or gas and particles (dry deposition). Once NO_x is released into the atmosphere it can react with water vapor to form nitric acid (HNO₃), which can be transported thousands of kilometers before being deposited as acid rain. The resulting acidification of the soil and waterways is harmful to the vegetation and aquatic wildlife, and has caused severe environmental problems in many parts of the world [4]. Emissions of sulfur oxide (SO_x) also cause acid deposition (in the form of H₂SO₄). However, SO_x emissions have been efficiently controlled during the last few decades by desulfurization and flue gas cleaning, and the problem of acid deposition has been resolved in many locations. Thus, in industrialized countries, acid rain is now mainly caused by NO_x emissions.

2.2 NO_x legislation

Although NO_x may form naturally, e.g., during lightning [5], anthropogenic activity is the main cause of increased NO_x levels in the atmosphere [6]. Most NO_x originates from combustion processes in which nitrogen in the air or in the fuel reacts with oxygen to form NO_x (discussed in detail in Chapter 3). In developed countries, NO_x emissions originate essentially from the

transport sector and/or the industrial sector, and the regulatory frameworks for NO_x emissions are important for these sectors. As this thesis deals with NO_x emissions from an industrial process, the transport sector (i.e., road vehicles, ships, and airplanes) will not be considered in this work.

In 1979, the Convention on Long-range Transboundary Air Pollution (CLRTAP) was signed by a group of 32 countries, which has today grown to include 51 countries worldwide [7]. The motivation for the convention was the rapid destruction of forests and entire ecosystems in European countries by acid rain from air pollution that originated thousands of kilometers away from the affected areas. The convention has been extended by several protocols, of which the Gothenburg protocol (1999) is the most recent [8]. This protocol aims by Year 2010 to reduce tropospheric ozone and the eutrophication and acidification of waterways by setting a limit on emissions of SO_x, NO_x, volatile organic compounds (VOC), and ammonia (NH₃). The protocol was entered into force in Year 2003, and was revised in Year 2012 to achieve further reductions in these emissions by Year 2020. Within the European Union (EU), directives are launched to set limits as to how much each Member State may emit. The individual countries then regulate the emissions on a national level. The latest EU directive regarding air pollution is Directive 2016/2284/EU [9], which entered into force on the 31st of December 2016; it states that NO_x emissions should be reduced by 42% by Year 2020 and 63% by Year 2030, relative to the levels of emissions in Year 2015. Figure 1 shows the annual emissions of NO_x and SO_x for the EU-15 countries and EU-28 countries, together with the limits set by EU directives to comply with the Gothenburg protocol [8-10]. The levels of NO_x and SO_x emissions have been reduced over the past 20 years, although the reduction of NO_x levels has been less successful. It is also clear that further reductions in NO_x levels are needed to reach the targets, while for SO_x immediate action is less urgently needed.

Apart from complying with national regulations to fulfil the targets set by Directive 2016/2284/EU, combustion plants within the EU also need to follow other directives. Large combustion plants (≥ 50 MW_{th}) are required to operate in accordance with the stipulations of a permit, which include an emission limit that is based on the use of best-available technologies (BAT) [11]. In practice, the processes are thereby obliged to implement BAT in order to be operational. However, it should be noted that the definition of BAT considers that the cost for controlling emissions should be proportionate to the environmental benefit. Medium-sized combustion plants (i.e., 1-50 MW_{th}) operate under a directive (the Medium Combustion Plant Directive; MCPD) that entered into force in December of 2015. The limits set by MCPD should be reached by Year 2018 for new plants and by Year 2025 or Year 2030 for existing plants (depending on size) [12].

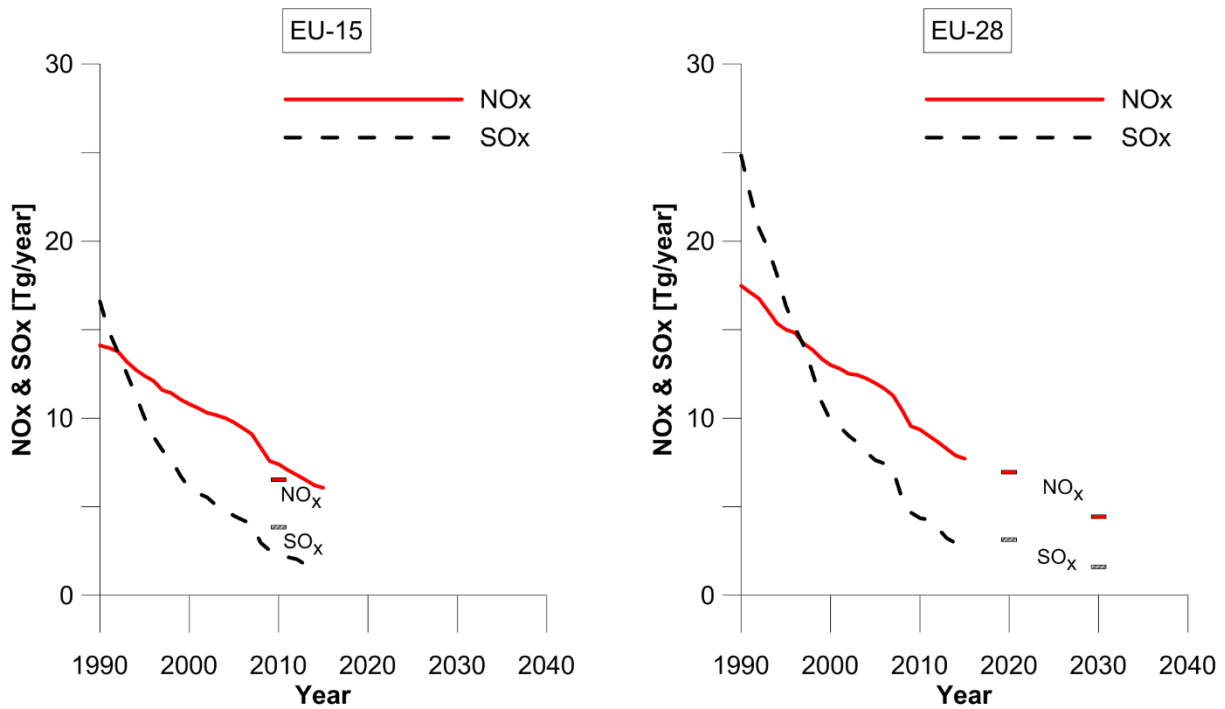


Figure 1. NO_x and SO_x emissions per annum for the EU-15 and EU-28 countries [10]. The target goals for NO_x and SO_x emissions set by the EU [8, 9] are also shown indicated by the respective boxes.

The environmental protection agency in Sweden (*Naturvårdsverket*) is the main authority responsible for reducing national emissions and they monitor the current status of emissions and evaluate possible improvements. They also provide information and support for legislation, which is finally decided upon by the Swedish Parliament. In 1992, a fee was imposed on NO_x emissions from energy-generating plants, with the consequence that NO_x emissions have decreased continuously since then [13]. The concerned companies are charged for their NO_x emissions and the revenue from this charge is then redistributed to the concerned companies in accordance with how much energy they have produced [14]. Plants that are not producing power or district heating are not affected by this fee, although they still have to comply with national targets. In general, the Swedish targets are more ambitious than the EU targets. For example, the NO_x limit for medium-sized combustion plants proposed by *Naturvårdsverket* is 300 mg/m³_n (at 6% O₂), as compared to the 650 mg/m³_n (at 6% O₂) limit set by the EU in the MCPD [15]. The monitoring of regional emissions is performed by the county governments (*Länsstyrelsen*), which may propose even stricter targets. *Länsstyrelsen* report yearly to *Naturvårdsverket*, which in turn reports to the Swedish Government.

Combustion-based power generation is relatively limited in Sweden, and most combustion occurs in other industrial processes or in car engines. In 1990, NO_x emissions from the transport sector accounted for about 55% and the industrial sector accounted for about 17% of the national NO_x emissions (the remainder is attributed to machinery, agriculture, and heat and power generation). In 2015, these values were 39% and 23%, respectively, although it should be noted that the absolute NO_x emissions have been reduced in both sectors, albeit more so for the transport sector. The iron ore industry, which is the focus of this thesis, is a substantial emitter of NO_x. The iron ore industry in Sweden typically has processing plants with a heat input of around 40 MW and will, therefore, most likely have to comply with the above-

mentioned MCPD. However, limited research has been carried out on NO_x mitigation measures for these plants. In these plants, the combustion conditions (which will be discussed later) differ from conventional combustion systems, and implementation of, for example, flue gas cleaning (SCR), is less efficient and more costly. With respect to iron ore pelletizing plants, the document that relates to BAT for iron and steel production [16] states that: “*Due to high costs, the end-of-pipe nitrogen oxide reduction of waste gas should only be considered in circumstances where environmental quality standards are otherwise not likely to be met*”. The proportionate cost for the environmental benefit is thus still being discussed for this industry. Therefore, there is an incentive to develop cost-efficient means to reduce the NO_x emissions from these plants. This necessitates an improvement of the current understanding of the relevant NO_x formation mechanisms in rotary kilns.

2.3 Iron ore production

Global steel production has grown from 189 million metric tonnes in Year 1950 to 1630 million metric tonnes in Year 2016, with half of this growth having occurred since Year 2000 [17]. Since steel production requires iron ore, it is reasonable to assume that iron ore will continue to be an importance product, although its production has declined slightly since Year 2014 [18, 19]. Australia is the leading producer of (useable) iron ore, followed by Brazil and China. Sweden produces around 1% of the world’s useable iron ore.

Steel blast furnaces typically require iron ore that has an iron content of at least 58% and that is in a form that allows the formation of a bed through which gas can flow with low resistance. Therefore, the mined iron ore is often concentrated and shaped into spherical pellets. The concentration process for iron ore involves removing impurities through grinding, filtration, and the addition of chemicals. This results in a slurry that is then formed into soft pellets (so-called ‘green pellets’), which are heat-treated before shipping. The heat treatment, which includes drying, oxidation, sintering, and finally cooling of the pellets, can be performed either in a ‘Straight-Grate’ process or in a ‘Grate-Kiln’-process. In the Straight-Grate process, the soft pellets are heat-treated in a bed upon a moving grate. In the Grate-Kiln process, the pellets are first dried and strengthened on a moving grate before being sintered in a rotary kiln. The focus of the current work is on the Grate-Kiln process, a detailed description of which is given below.

A schematic of the Grate-Kiln process is shown in Figure 2. While different plants may have slightly different configurations, the overall layout is similar. The green pellets are fed onto the grate where they are dried and preheated by the recirculated hot air flows from the cooler. The grate is divided into zones that receive air from a corresponding zone in the cooler. If the iron ore contains substantial amounts of magnetite (Fe₃O₄), a significant level of heat is released by the oxidation to hematite (Fe₂O₃), which begins in the later stages of the grate (TPH and PH). By the time they reach the end of the grate, the pellets are of sufficient strength to be introduced into the rotary kiln, where they are sintered. The kiln is slightly tilted, so that the pellets gradually move forward under gravity, and due to the kiln rotation the pellets are thoroughly mixed, so that uniformity of the final product is achieved. The heat required for sintering is transferred to the pellets by a flame, usually involving the combustion of coal, although oil and gas are also used. The hot sintered pellets then proceed to the cooler where they are cooled by

ambient air. The warm air that exits the cooler is used for preheating the pellets on the grate and as combustion air in the kiln. The air used in the kiln comes from the first part of the cooler (C1 in Figure 2) and may have a temperature of $>1100^{\circ}\text{C}$, which is significantly higher than the temperature of the combustion air in heat and power generation plants. Although most of the oxidation of the pellets occurs on the grate, it is important to maintain high levels of oxygen in the kiln, to ensure a high degree of oxidation, and to prevent reduction back to magnetite. Thus, a large volumetric flow of air from C1 is needed. Relating the air flow to the fuel flow, an air-to-fuel equivalence ratio of 4-6 is obtained in the kiln, which is significantly higher than the equivalence ratio (approximately 1) in conventional solid fuel combustion.

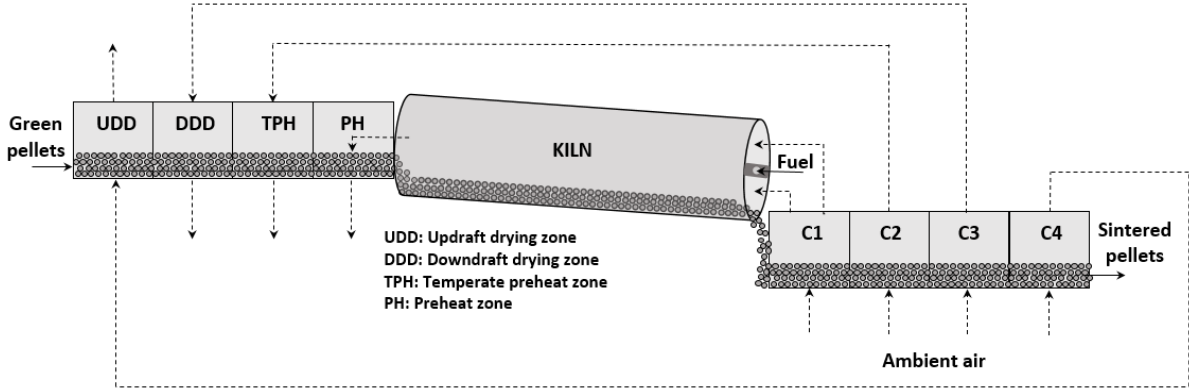


Figure 2. Schematic view of the Grate-Kiln process. The dotted lines indicate the air flows through the process.

3 Theory

Combustion is a complex process that involves numerous chemical reactions. For simplicity, the written formulas often only include the initial reactants and final products. An example of this is the complete oxidation of methane:



In reality, thousands of intermediate reactions occur, involving hundreds of intermediate species (CH₃, OH, HO₂, CO etc.). Some of these species are relatively stable (e.g., CO), while others are unstable (e.g., OH) and react rapidly with other compounds. The unstable species are mainly radicals (i.e., they have an unpaired valence electron), and they are crucial to understanding the progress of combustion. Radicals also govern the formation of NO_x during combustion. The main elements of solid fuel carbon (C) and hydrogen (H) will end up as CO₂ and H₂O regardless of how the combustion progresses, as long as combustion is complete. However, nitrogen (N) may be converted to NO_x or N₂ depending on the progress of the combustion process and the distribution of radicals. The composition of the radical pool is dependent upon the kinetics of the relevant reactions, which in turn are dependent upon the rate constants and the availability of reactants. The rate constant is commonly described by the modified Arrhenius expression:

$$k = AT^n e^{-\frac{E_a}{RT}} \quad \text{Eq. 1}$$

where k is the rate constant, A and n are constants that describe the pre-exponential factor, T is the temperature, E_a is the activation energy and R is the gas law constant. For many reactions, n is assumed to be zero. Mathematically, this expression gives that the rate constant (and thus the reaction rate) increases exponentially with temperature, as long as the activation energy is not zero and the temperature is less than the value of $E_a/2R$. A high activation energy results in low rates at low temperatures. This expression is the most common way to express chemical reaction rates, although other expressions exist, for example, surface reactions.

NO_x is dominated by NO at the high temperatures involved in combustion processes. Therefore, research on NO_x is concerned with the formation and destruction of NO rather than NO₂. However, the emitted NO rapidly converts to NO₂ at lower temperatures. This chapter describes the NO chemistry during combustion and discuss the influences of combustion parameters. The focus here is on solid fuel combustion, as solid fuels are the most commonly used in the Grate-Kiln process.

3.1 NO formation routes

NO can be formed from either the nitrogen gas (N₂) introduced with the air or the nitrogen introduced with the fuel (fuel-N). When firing gaseous or liquid fuels, it may be assumed that all the generated NO originates from N₂, due to the absence or low level of fuel-N. In contrast, fuel-N is usually the main contributor to NO in solid fuel combustion [20]. Although NO

formation is complex and includes hundreds of intermediate reactions, it is – for pedagogic reasons – common to split the process into three mechanisms:

- Thermal NO formation – reaction between N_2 and O_2 to form NO
- Prompt NO formation – reaction between N_2 and fuel radicals to form NO
- Fuel NO formation – oxidation of fuel-N to form NO

Thermal NO formation, as the name suggests, is important only at high temperatures, since the N_2 molecule contains a strong triple bond that requires large amounts of energy to break. The mechanism is referred to as the Zeldovich mechanism [21]. Originally, it involved the two reactions R 3-2 and R 3-3 while the third reaction R 3-4 was added later.



Thermal NO formation is limited by the forward reaction of R 3-2, and once activated, it fuels the other reaction by providing N-radicals. The activation energy of R 3-2 is approximately 318 kJ/mol. Typically, the formation rate of thermal NO becomes significant, relative to other NO reactions, at around 1500°C, although the concentrations of O_2 and N_2 and NO are also important in determining the resulting rate. The gas residence times at these high temperatures are also important in terms of the total amount of NO produced *via* the thermal mechanism.

Prompt NO formation converts N_2 into NO through an initiating reaction between a hydrocarbon radical and an N_2 molecule. The number of relevant reactions far exceeds the reactions involved in thermal NO formation, which means that prompt NO formation is significantly more complex. While prompt NO formation is rapid (hence its name), it is only active in the presence of short-lived hydrocarbon radicals. It can play an important role in hydrocarbon flames, although it has been shown to have a negligible role when fuel-bound nitrogen is present. This thesis focuses on solid fuel combustion (with fuel-bound nitrogen), so prompt NO will not be explicitly considered.

Fuel-N conversion is discussed in detail in the next section. In summary, the fuel-bound nitrogen ends up either as NO or N_2 , depending on the local conditions during the combustion process. In particular, the air-to-fuel equivalence ratio, λ , is important for fuel-NO formation. Considerable progress has been made in understanding fuel NO formation. However, this type of formation includes many different processes and is, to say the least, challenging to describe. Empirical data are still needed to describe the formation, especially regarding the interaction between the solid and gaseous phases.

Although categorizing NO formation in this manner is convenient, these are not mutually exclusive mechanisms. An illustrative example is R 3-2, which ably describes thermal NO production as long as there are no other sources of NO. However, when NO is already present (from, for example, the oxidation of fuel-N) the equilibrium of this reaction will be shifted to the reactant side in line with Le Chatelier’s principle, thereby reversing the reaction. This is

mentioned in the review of Glarborg [22] with reference to the work of Pershing and Wendt [20], and temperatures as high as 2200 K could be required for thermal NO to contribute significantly when coal dust flames are used. Given these types of interactions, determining the contribution of each NO mechanism to the total NO formation is not a trivial task.

3.2 Fuel-N evolution during solid fuel combustion

A solid fuel particle undergoes several processing steps during combustion. In a pulverized fuel (PF) flame, the particle is heated through convection and radiation from the upstream flame as well as the walls, and the water contained in the particle starts to evaporate. For small particles, as in PF flames, this process occurs rapidly (takes a couple of milliseconds). Once the drying is completed, the particle temperature increases, the particle starts to decompose, and volatile compounds contained in the particle escape from the solid fuel matrix. This process is called ‘devolatilization’ or ‘pyrolysis’, depending on whether oxygen is present or not. For bituminous coal particles, significant pressure builds up inside the particle, which causes it to swell or fracture. The products of devolatilization are volatiles and char. The volatiles, which comprise light-weight gases (such as CO and CH₄) and tars (heavier hydrocarbons), react with oxygen to form a small flame envelope around the remaining particle. The processes of devolatilization and volatile combustion occur on a time-scale similar to that of the drying process. The solid fraction of the particle remains after devolatilization is called ‘char’, and it consists mainly of carbon and ash, although small amounts of other elements are also present. When the combustion of volatiles is complete and the flame envelope is gone, oxygen reaches the surface of the char and may diffuse into the pores. Heterogeneous reactions between the solid and the gaseous oxygen occur, and the products consist mainly of CO and CO₂. The time-scale for char combustion is considerably longer than those of the previous processes, and usually takes hundreds of milliseconds to reach completion.

The fuel-bound nitrogen is released either with the volatiles or with the char, and the conversion to NO or N₂ will depend on the local conditions. The following sections will cover the partitioning of nitrogen between volatiles (vol-N) and char (char-N), followed by an examination of the formation of NO from vol-N and char-N. Thereafter, the reduction of NO is discussed.

3.2.1 Nitrogen partitioning during pyrolysis

The partitioning of nitrogen during pyrolysis is important for NO formation, since the combustion process and the possibility for NO_x control differ substantially between volatile- and char-bound nitrogen. Different conditions yield different volatile products, and there is consensus regarding the importance of the pyrolysis temperature in dictating the amount of fuel-N that is retained in the char. Figure 3 presents the amounts of nitrogen that are lost with the volatiles during pyrolysis, based on the works of Zhang and Fletcher [23], Blair et al [24], Pohl et al [25], Solomon and Colket [26], and Kambara et al [27]. Even though there is a clear trend towards more nitrogen leaving with the volatiles at higher pyrolysis temperatures, there are considerable differences between the test series. Blair et al [24] also compared the release rate of nitrogen to the release rate of total mass (which also increases with temperature) during

pyrolysis, and concluded that nitrogen release is more sensitive than mass release to temperature.

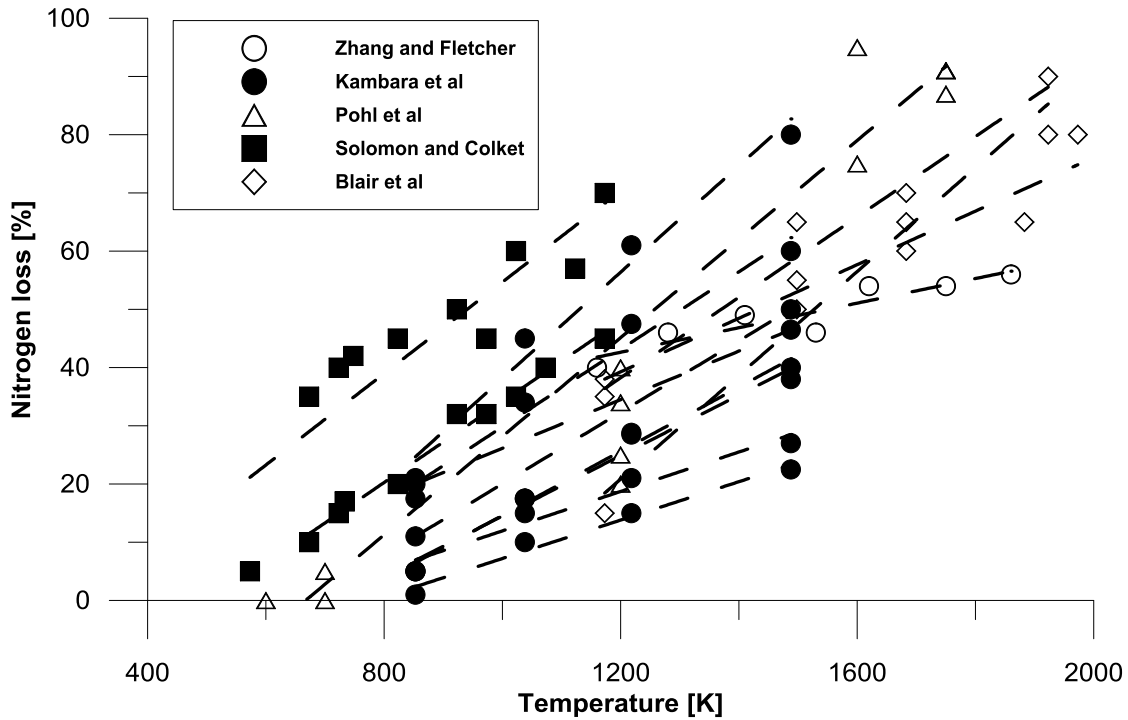


Figure 3. Nitrogen loss as a function of pyrolysis temperature. The data are taken from the indicated publications in the literature [23-27]. Trend lines are shown for each investigated coal.

As seen from the wide range of data-points in Figure 3, the fraction of nitrogen that leaves with the volatiles is not predictable when it is based solely on the pyrolysis temperature. Kambara et al [27] have stated that it is impossible to predict the partitioning of volatile nitrogen based on proximate and ultimate analyses, as they found that two coals with the same levels of nitrogen and volatile matter yielded two different fractions. However, since then, several models have been developed with reasonable success to predict the composition and yield of volatiles based on the chemical structures of coals. Three commonly used pyrolysis models are FG-DVC [28], FLASHCHAIN [29], and CPD [30].

3.2.2 Vol-N conversion

The nitrogen-containing volatiles (vol-N) evolve mainly as light-weight nitrogen species (HCN or NH_3), either directly from the coal matrix or indirectly from the tar formed during pyrolysis, and thereafter reacts with radicals to form either NO or N_2 . The conversion of light-weight nitrogen gas species to NO is largely dependent upon the availability of oxygen. The conversion varies from 0% to 100% depending on the local stoichiometry (i.e., oxygen-rich or oxygen-lean) [25, 31]. Thus, if left uncontrolled, vol-N can be a significant contributor to total NO formation. Given that local stoichiometry has such a significant impact, it is beneficial to design burners and combustion equipment to achieve oxygen-lean combustion zones, so as to reduce net NO formation. Miller and Bowman [32] have provided a thorough assessment of the oxidation of light-weight nitrogen species, and the major reaction pathways for HCN and NH_3 have been confirmed: nitrogen atoms in HCN or NH_3 end up as N radicals, which then react either with OH to form NO or with NO to form N_2 . In other words, when N radicals are formed,

the reactions with NO and with OH compete to form either N₂ or NO. The rate constants of these reactions are usually of similar magnitude, and the yield of NO and N₂ is, thus, a function of the ratio between the OH and NO concentrations.

Several detailed reaction mechanisms have been proposed for the homogenous interaction between hydrocarbon combustion and NO formation. The best-known mechanism is the GRI-Mech mechanism [33], which has been widely used and refined in more recent studies. Such detailed mechanisms are capable of describing the premixed gas flame chemistry with high accuracy. A common approach is to assume that all of the vol-N is released as HCN or NH₃ and thereafter converted to NO and N₂, depending on the local gas-phase conditions.

Nitrogen-containing volatiles that are not directly released from the coal matrix or from the tar will be incorporated into the soot (soot-N) formed by the tar. The reported values for the fractions of volatile nitrogen components trapped in the soot are generally low, even though they may reach up to 30% [34, 35]. The fate of soot-N is not well understood. Soot itself can effectively reduce the level of NO [36, 37], although incorporated soot-N means that there are lower concentrations of light-weight nitrogen gas species susceptible to primary NO_x reduction measures.

3.2.3 Char-N conversion

Since it is possible to control the conversion of vol-N to NO using controlled mixing of the oxygen and fuel, the oxidation of char-N has grown in importance relative to NO formation. Phong-Anant et al [38] used a drop tube reactor at different temperatures and stoichiometric ratios, and found that under “normal” conditions for PF combustion ($\lambda = 1.4$, $T = 1673$ - 1773 K), char-N contributed to around 40% of the total NO formation. In the case of fuel-rich combustion ($\lambda < 1$), the contribution of char-N was 60%-90%. Although char-N conversion has been extensively studied, the results are non-conclusive. A challenge is to differentiate between intrinsic char-N conversion, i.e., the selectivity of char-N towards NO (prior to reduction by the char), and apparent char-N conversion, i.e., the net conversion after NO reduction by char has occurred. As NO is usually measured when the combustion process has finished, data for apparent char-N conversion data are more common in the literature than data for intrinsic char-N conversion. Table 1 presents several char-N conversion values obtained under conditions relevant to flame combustion. The values vary in the range of 10%-100 %. Different authors have provided different reasons for this variability. Most of the experimental studies [39-43] have noted an increase in char-N conversion with increasing level of oxygen, the magnitude of the observed increase varies between studies. Jensen et al [44] found that the conversion of char-N to NO was close to 100% when very small samples of char (<1 mg, to minimize the NO-char reduction) were combusted at 1323 K and 1423 K, whereas for combustion at 1123 K the conversion of char-N to NO was 65%. The conversion rate decreased rapidly when the sample size was increased. The availability of O₂ did not affect the conversion rate for small samples. These results imply that the intrinsic char-N conversion is 100%, and that NO reduction by char is responsible for the lower values of char-N conversion. Molina et al [42] also found a decrease in char-N conversion when the char sample size was increased (≈ 4.5 - 21.0 mg). Furthermore, they performed two types of experiments that resulted in two significantly different levels of char-N conversion. In the first (Type I) experiment, the char was first injected

into a helium atmosphere and pyrolyzed (low levels of NO and CO exited the char) for 60 s, and then an O₂/He mixture was injected to facilitate combustion. In the second (Type II) experiment, the char was injected directly into a stream of O₂/He. The Type I experiments resulted in char-N conversion values in the range of 10%-15%, while the Type II experiments gave values in the range of 40%-55%. The authors attributed this difference to the lower local stoichiometry used in the Type I experiments leading to an increase in the homogenous reduction mechanism that involves HCN. The importance of HCN for char-N conversion is not established, although modeling conducted by some groups (see for example [45, 46]) have shown that assuming HCN to be the primary product from char-N provides good results. Another common approach is to use NO as the primary product obtained from char-N, with subsequent reduction by char.

Additional combustion issues are discussed by Shimizu et al [47], who showed that the conditions during char production affect the final conversion of char-N to NO, and Spinti and Perching [40] have taken this as an explanation for the differences observed in the literature. Jensen et al [45, 46] have shown that NO-char reduction is significantly faster directly after pyrolysis than when the char has been prepared separately, as is the case in most NO-char reduction studies.

Table 1. Experimental values for char-N conversion to NO relevant to PF combustion, as taken from the literature.

Authors	Apparatus	Set temperature [K]	Char-N conversion (%)
Perching and Wendt [41]	Combustor		10-15
Spinti and Perching [40]	Combustor		40-60
Nelson et al [43]	Combustor		35-80*
Song et al [39]	EFR	1250-1750	20-35*
Molina et al [42]	EFR	1698	10-55
Phong-anant et al [38]	EFR	1273-1873	30-50
Pohl et al [25]	EFR	1500	1-20*
Wang et al [48]	EFR	1273	10-45
Jensen et al [44]	Fixed bed	1123-1423	10-100

* Only values for $\lambda > 1$ are taken. Lower values were obtained when λ was < 1 .

EFR: Entrained Flow Reactor (includes drop tube reactors).

As char-N conversion is closely linked to char conversion, a brief overview of char combustion is presented here. Char combustion may be divided into three zones based on the limiting rate. In Zone I, the char conversion rate is kinetically controlled and increases rapidly with temperature. In Zone III, the rate is controlled by the mass transport of oxygen to the char and is less dependent upon the temperature. Zone II represents conditions in which both kinetic and oxygen transport rates are important. High temperatures move the combustion towards Zone III, since the chemical reaction rates increase, making mass transport the limiting factor. In contrast, using small particles moves the combustion towards Zone I, as the specific diffusive mass flux to the particle is increased, thereby promoting more rapid mass transport. High temperatures and small particles are present in pulverized coal combustion, and these systems are generally well represented by the conditions characteristic of Zone II [49]. Due to the abovementioned factors, it is clear that it is complicated to describe char oxidation over a wide range of temperatures and combustion conditions, especially with respect to the partial pressure

of oxygen. In general, neither global power-law kinetics nor semi-global Langmuir-Hinshelwood kinetics describe with sufficient accuracy the temperature dependence. Instead, more complex models are required, some of which attempt to maintain the dependence on just temperature and concentrations [50], while others include dimensionless numbers and specific coal parameters [51].

3.2.4 NO reduction

Since it is most common to report the values for apparent char-N conversion, which is primarily a function of NO reduction by char if the intrinsic char-N conversion is 100%, it is worthwhile to discuss the NO reduction mechanisms. It is convenient to divide the NO reduction process during solid fuel combustion into reduction by volatiles and reduction by char, as these reactions occur on different time-scales. NO reduction by volatiles is important and is the main reason why air staging achieves significant reductions in NO, i.e., by prolonging the zone in which NO can interact with the radicals formed by the volatile compounds. This mechanism is also used when fuel staging is applied, i.e., introducing a fuel (e.g., natural gas) downstream of the initial combustion zone. The reduction of NO may occur by reaction with N-containing species (such as NH_i) or N-free species (such as CH_i) [52]. In those combustion systems in which fuel staging is not applied, NO reduction by volatiles only affects the NO formed during the early stage of combustion, while the NO formed subsequently is not affected.

In contrast, the reduction of NO by char affects a larger fraction of the formed NO, since the char reactions occur on a longer time-scale. Many studies have been conducted on NO reduction by char and carbonaceous materials, and several of those studies have suggested a decrease in the apparent NO conversion as the background NO level is increased, i.e., the $(\text{NO}_{\text{out}} - \text{NO}_{\text{in}})/\text{char-N}$ ratio decreases significantly as the initial NO concentration increases [40, 42, 45, 53]. Some of these studies have even observed negative rates of apparent conversion of char-N, i.e., more NO is reduced by the char than is formed by the char-N [40, 45]. This reduction appears to be enhanced in the presence of CO [46]. Aarna and Suuberg [54] have reviewed the studies on NO-char kinetics in the literature and averaged the rates; the resulting rate constant is shown in Figure 4 along with selected constants. Most of the rates found in the literature are within one order of magnitude of the Aarna and Suuberg rate. However, most of the studies have used chars that have been prepared prior to the experiments. Jensen et al [44] have shown that the rate of NO-char reduction decreases continuously in the time-span after pyrolysis, due to some deactivation mechanism, and that the rate directly after pyrolysis is significantly higher than that usually reported in studies in which the chars have been prepared separately. The rate reported by Song [55] is included in the figure, since it was obtained from experiments performed in the temperature range relevant to the conditions in a rotary kiln. The rate reported by Jensen et al [44] is shown for comparison, and this rate is also applied in the modeling of this thesis. While it is significantly higher than the average rate provided by Aarna and Suuberg [54], it is derived in one of the few studies in which the char was produced *in situ* with NO-char reactions proceeding directly afterwards. The rate described by Chan [56] was obtained at lower temperatures. Nonetheless, it is recommended by Visona and Stanmore [46] for pulverized fuel combustion carried out at around 1750 K. Extrapolating this rate to higher temperatures results in a rate similar to that found by Jensen and co-workers. Finally, it should

be mentioned that Molina et al [45] increased by one order of magnitude the rate of Aarna and Suuberg, to achieve fitting to their experimental data, which further indicates that the NO-char rate is higher than what is usually found in the literature, and that the rate reported by Jensen et al [54] is a strong candidate for describing the NO-char reduction in a PF flame.

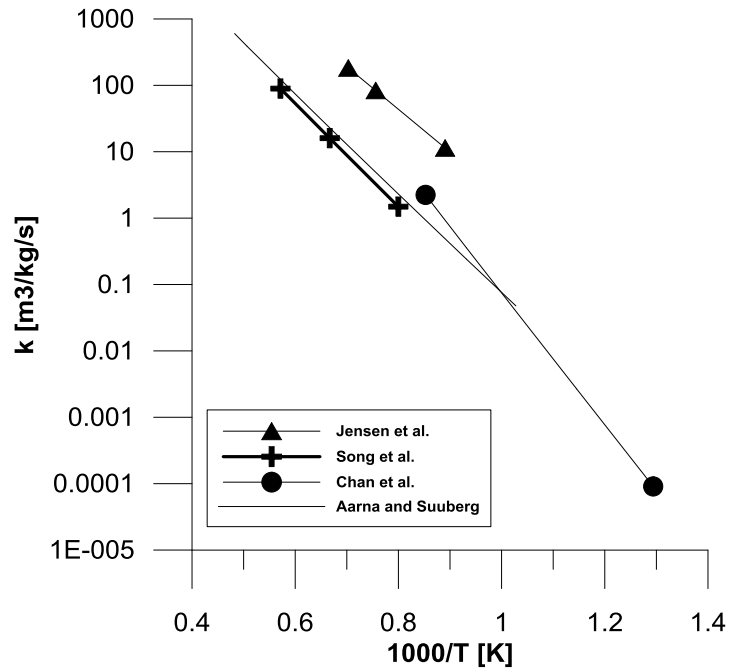


Figure 4. Arrhenius plot of the NO-char reaction. The rates (in $\text{m}^3/\text{kg}/\text{s}$) are derived from Song et al. [55] and Aarna and Suuberg [54] assuming a char surface area of $150 \text{ m}^2/\text{g}$. An area of $530 \text{ m}^2/\text{g}$ was used for the Chan rate [56]. The rate of Aarna and Suuberg is an average rate and does therefore not include any symbols.

3.3 General NO_x mitigation strategies

3.3.1 Air staging

The most commonly used measure to reduce NO_x is to control the mixing of the air and the fuel to create an oxygen-lean zone during vol-N conversion, thereby yielding a lower rate of NO formation from volatile nitrogen. Mixtures that are overly oxygen-lean may, however, result in flame extinction. Burners are typically built with two registers for air: primary and secondary. The primary air may be premixed with the fuel or mixed rapidly. The secondary air is usually added through an outer register and is most often swirled, creating a reverse aerodynamic flow in the flame. Due to this reverse flow, hot (O_2 -lean) gases are recirculated to the early part of the flame, which is beneficial for NO reduction. Swirling may also be applied to the primary air. There tends to be an optimal NO_x emission level with regard to swirling, as a low rate of swirling will not result in a significant recirculation zone, while a too-high rate of swirling will mix the air with the fuel too rapidly and NO_x formation will increase. Staging air through burner design is called ‘internal staging’. It is also possible to stage the air externally by adding enough air through the burner to ignite the fuel, and adding the remainder at a later stage through separate ports (often called ‘over fire air’, OFA) (e.g., along the wall), to ensure burnout. For rotary kilns, OFA is not possible due to the rotation of the kiln.

3.3.2 Fuel staging

Introducing part of the total fuel input at a later stage in the combustor enables the formed NO to be reduced by, for example, hydrocarbon radicals (CH_i). The mechanism is called 'reburning', and it has proved to be an efficient way to reduce NO_x . The reburn fuel is typically natural gas, although solid fuels may also be used as long as they ignite readily and mix well. The reburn zone is generally sub-stoichiometric and additional air has to be added after this zone. Although fuel staging is generally performed externally, it is also possible to apply internal fuel staging using burners with different fuel registers.

3.3.3 Fuel switch

Since fuel-N is a significant contributor to NO formation in PF flames, a simple measure that is often used is to switch to a fuel that contains less nitrogen. Switching from a solid fuel to a gaseous fuel tends to decrease significantly the NO_x emissions. However, the linkage between the fuel-N content in solid fuels and NO emissions is weak, as fuel-N conversion depends on many other aspects. Thus, changing to a solid fuel with a lower nitrogen content does not guarantee a lower level of NO_x formation. The content of volatiles has, for example, been shown to play a significant role. In unstaged flames, a higher volatile content leads to higher NO emissions, whereas for staged flames the opposite trend is observed. The reason for this is that a fuel that has a high content of volatiles is likely to release more volatile nitrogen, and if air staging is achieved it will affect a larger fraction of the total fuel-bound nitrogen. Other fuel properties, such as particle size and ash content, can also play important roles, so it is difficult to predict the effect on NO of a fuel swap.

Another possibility is to co-combust the fuels. Apart from reducing the amount of incoming fuel-N, the interaction between the two fuels has the potential to create NO reduction by forming additional, local O_2 -deficient zones. In theory, a volatile fuel with low nitrogen content could be manipulated so that a reducing zone is formed at an optimum location, thereby reducing the fuel-N conversion from the other fuel [57]. Co-combustion also facilitates the combustion of certain fuels that may be difficult to ignite. Using a small amount of gaseous fuel can, for example, stabilize a solid fuel flame.

3.3.4 Other primary measures

The relationship between stoichiometry and NO formation is clear; a lower stoichiometry (air/fuel) results in a lower level of NO formation, which means that decreasing the overall excess of air an effective measure. Although it is always the local stoichiometry that determines the level of fuel-N conversion, the global stoichiometry controls the ease with which local O_2 -lean zones can be created. The stoichiometry in the early part of combustion can, as mentioned, be controlled effectively through burner design, whereas the stoichiometry in the later stages is less sensitive to such changes. However, decreasing the global stoichiometry lowers the O_2 levels post-flame inherently.

Another possibility is to recirculate the O_2 -lean flue gases through the burner. This has three potential benefits for NO reduction: the reduction in O_2 concentration leads to decreased oxidation of fuel-N, as well as a lower temperature (reducing the thermal-NO mechanism), and the recirculation enables a reduction in the NO levels through reburning. Substantial reductions

in NO levels have been attained in oil- and gas-fired boilers owing to the decrease in thermal-NO formation, while this strategy has proven to be less effective for solid fuels [58].

3.3.5 Secondary measures

If NO_x emissions cannot be reduced effectively using primary measures, flue gas cleaning may be necessary. This is performed by adding ammonia (NH₃), which reacts with NO to form N₂. Urea [CO(NH₂)₂] is also used, since it decomposes to NH₃ but is safer to handle. The reaction between NO and NH₃ is highly temperature-dependent, and it is most efficient at temperatures in the range of 900°-1100°C. At higher temperatures, the oxidation of ammonia becomes more prominent, which can result in increased NO emissions, while at lower temperatures, the reaction may not proceed to completion and ammonia may be emitted (so-called ‘ammonia slip’).

The reduction of NO by NH₃ is possible at lower temperatures (200°-500°C) if a catalyst is present. This is selective catalytic reduction (SCR), and it can provide significant NO_x reduction. The reduction without a catalyst is called selective non-catalytic reduction (SNCR) and is less common in industrial systems.

3.4 Units of emission measurements

Several units for quantifying NO_x emissions are used depending on application. A common unit in research is the volumetric gas fraction of NO_x given in ppm as it is the unit employed by most measurement instruments. The volumetric gas fraction is equivalent to the molar gas fraction and proportional to the partial pressure and concentration. The latter is, however, dependent on system conditions like pressure and temperature. The concentration and partial pressure are useful units as they determine the rate of reactions. It may also be of interest to look at the ratio of emitted NO_x to introduced fuel-N, since this relates to the performance of the combustion process with regard to NO_x emission. The NO_x to fuel-N ratio is used in Papers I and II.

Neither of these units directly quantifies the amount of NO_x formed in the process as they depend on the flue gas flow. A common approach to avoid this is to correct NO_x fraction to a certain base oxygen level. This correction is performed according to:

$$x_{NO_x,corrected} = x_{NO_x} * \frac{x_{O_2,ox} - x_{O_2,base}}{x_{O_2,ox} - x_{O_2}} \quad \text{Eq. 2}$$

where $x_{NO_x,corrected}$ is the corrected molar NO_x fraction, x_{NO_x} is the measured molar NO_x fraction, x_{O_2} is the measured molar O₂ fraction, $x_{O_2,ox}$ is the oxygen molar fraction in the oxidizer (≈0.21 for air), and $x_{O_2,base}$ is the base oxygen fraction to which the emission should be corrected (0.06 for solid fuels within the EU).

It is also common to use the unit mg_{NO2}/m³_n instead of the molar fraction. This unit is equivalent to the molar fraction and the conversion is obtained by applying the ideal gas law and assuming that all the NO is converted to NO₂. Correction to a base oxygen level might still be necessary, and it is also performed using Eq. 2.

Another common practice is to relate the emitted NO_x to the energy input, i.e., $\text{mg}_{\text{NO}_2}/\text{MJ}_{\text{fuel}}$. An advantage of using this unit system is that correction to a certain oxygen level is not needed. It does, however, depend on accurate measurements of the flue gas flow and the fuel feed, which are not always available. Attention must also be paid to the specific heating value (lower or higher) on which the unit is based.

For the Grate-Kiln process, use of the molar fraction or $\text{mg}_{\text{NO}_2}/\text{m}^3_n$ corrected to a certain oxygen level should be avoided, as the product (the pellets) absorb a certain amount of oxygen, thereby introducing an error when attempting to correct the NO_x measurement (see Appendix A for proof). Nonetheless, this approach is used in Paper I for comparison with European emission legislation, as there were no pellets present in the pilot-scale kiln used in the experiments. A unit that is commonly used in industrial production processes is $\text{NO}_x/\text{unit of production}$. In the Grate-kiln process, this is expressed as $\text{g}_{\text{NO}_2}/\text{tonne pellets}$, and it may be advantageous because it incorporates the production efficiency of the plant. It is, however, difficult to compare NO_x emissions across different industries using this unit system.

Units corrected to a certain oxygen level or related to the energy input are often used in legislation aimed at industrial applications; the review of Baukal and Eleazer [59] provides more details. Finally, it should be noted that these units indicate the environmental performance of individual plants, and that using them in designing legislation incentivizes the use of BAT. The environmental impact on a regional or global level is, however, more sensitive to the absolute amount of NO_x emitted than to the concentrations in flue gases, i.e., for evaluating the degree of pollution, $\text{kg}_{\text{NO}_2}/\text{year}$ is superior to $\text{mg}_{\text{NO}_2}/\text{m}^3_n$. The Gothenburg protocol and Directive 2016/2284/EU use units of $\text{kton}_{\text{NO}_2}/\text{year}$.

4 Previous work on NO_x in rotary kilns

In addition to their application in iron ore manufacturing, rotary kilns are used in cement production, lime manufacturing, lightweight aggregate manufacturing, reduction of oxide ore, and waste incineration [60]. The most common application is in the cement industry, and most of the research on combustion in kilns has been performed using cement kilns. This section provides an overview of the research on cement kilns and on the iron ore kiln. It should be noted that although both industries use rotary kilns, there are significant differences in terms of their design and use: sintering cement clinker requires a bed temperature of about 1450°C and the flue gas oxygen concentration is 2%-4%, whereas iron ore is sintered at around 1300°C and employs a level of excess air equivalent to 15%-17% oxygen in the flue gases.

4.1 Cement industry

Among the various studies of NO_x control in cement manufacturing, there is a consensus that thermal NO formation dominates NO formation in the rotary kiln, and intensive efforts have been made to reduce the levels of NO_x in other parts of the process (specifically, the precalciner). However, emissions-related legislation has motivated research also on the kiln. Vaccaro [61] reviewed NO_x campaigns conducted in industrial cement kilns and concluded that significant NO_x reductions could be achieved through the use of low-NO_x burners. In kiln systems, these burners have two primary air inlets (one is swirling and one is axial) and one fuel inlet. The amount of primary air used was considered to be especially important. The NO_x emission levels could be reduced by 45% (compared to a mono-channel burner) by lowering the amount of primary air while maintaining stable operation. Further reductions could be achieved (up to 54%), although this entailed unstable operation. In a review performed by McQueen et al [62], decreasing the level of primary air was shown to have the potential to reduce NO_x levels by 30%. Other primary measures were found to contribute NO_x reductions of 15%-30%, while the use of SNCR and SCR could reduce NO_x levels by 40%-70% and 70%-90%, respectively.

Both the European Union and the US Environmental Protection Agency have published documents on NO_x control in the cement industry that include several proposed measures [63, 64]. One measure that is unique to rotary kilns is a fuel switch from gas to coal. A gas-fired cement kiln could achieve a decrease of up to 70% in NO_x emissions by switching the fuel to coal [63]. Reducing the amount of excess air (i.e., the flue gas oxygen concentration is reduced from 2% to 1%) was shown to decrease the levels of NO_x by 15%. An innovative NO_x strategy that has been discussed is fuel staging by means of “mid-kiln firing”, which entails the use of a fuel inlet through the wall half-way along the rotary kiln. This allows slow-burning fuels, such as whole tires, to be introduced once per rotation of the kiln. Since the energy input by the kiln inlet can be reduced by this measure, the combustion is dispersed and the level of NO_x is reduced by as much as 50%. The use of low-NO_x burners does not always yield reductions in NO_x, but the reported values are up to 35%.

4.2 Iron ore industry

A limited amount of research has been performed on the emissions performance of iron ore rotary kilns, and many aspects are assumed in the literature to be shared with cement rotary kilns. In rotary kilns, firing with natural gas has been shown (as in cement kilns) to produce more NO_x than firing with solid fuels [65], which underlines the importance of thermal NO formation. Similar to cement kilns, the high levels of NO_x emissions produced during solid fuel combustion are assumed to be the result of the dominance of thermal NO_x formation. As will be shown from the results in Chapter 7, this thesis questions this assumption and suggests that fuel-N contributes significantly more.

The modeling of a gas-fired rotary kiln for iron ore production performed by Davis [66] revealed a minimum level of NO production at a certain secondary air flow. A low level of secondary air flow resulted in a high level of NO formation due to the long residence times and high peak temperature (i.e., high thermal NO formation), while a high secondary air flow also resulted in high-level NO formation due to the increased O₂ levels, although the temperatures were reduced. Apart from this study and some general emission reports [67, 68], not much research is available on NO_x in rotary kilns for iron ore production.

Papers I and II of this thesis are the first published reports that specifically investigate NO_x formation in iron ore rotary kilns using solid fuels and in-flame measurements. However, previous (unpublished) work has been performed by LKAB in a project called ULNO_x (Ultra Low NO_x) using the same test facility as in Paper I, as well as full-scale experiments. Similar to the previously mentioned results, the NO_x emissions were significantly higher when natural gas was tested in pilot scale, as compared to the use of solid fuels. Burning oil resulted in emissions similar to those seen with natural gas. An issue with the project is that the pilot-scale kiln generally produced higher levels of NO_x than the full-scale kiln, which raises difficulties with transferring the results from the pilot-scale kiln to the full-scale kiln. Table 2 presents a summary of the tested NO_x reduction measures and their effect in pilot scale as well as in full scale (if tested). NO_x reduction of 25% was observed in the pilot kiln by using a low NO_x burner but significantly lower NO_x reduction was observed when applying it to full scale. Modifications to the inlet (called hood) of the secondary air have been performed both in pilot scale and in full scale but any significant NO_x reduction in full scale has not been achieved. Switching fuel has also been investigated in pilot scale (Paper I is the latest of these trials). Out of all alternative coals tested, lowest NO_x emission has always been achieved with the reference coal (Coal A). Co-combusting propane and coal did not increase NO_x. Heating of primary air, heating of coal, addition of water to the process and replacing the primary air with inert gases did not result in any NO_x reduction in pilot scale. Decreasing the secondary air temperature by about 100°C was shown to decrease NO_x emission by about 40% in pilot scale. The feasibility of isolating this parameter in full scale is however not straight-forward since the secondary air temperature is dependent on the cooling of the pellets.

Table 2. Tested primary measures in the ULNO_x project

Primary measure	Description	NO _x reduction pilot scale	NO _x reduction full scale
Low NO _x burners	12 different burners were tested	20-25%	0-12%
Kiln hood modifications	Less intensive mixing of secondary air	10-25%	<10%
Decrease in secondary air temperature	From 1080°C to 970°C	40%	Not tested
Heating of primary air	170°C	0%	Not tested
Heating of coal	85°C	0%	Not tested
Propane co-fire		0%	Not tested
Reducing excess air	7.5% reduction	Not tested	8.5%*
	55% reduction	17%	Not tested
	72% reduction	33%	Not tested
Reducing primary air	87% reduction	8.5%**	Not tested
Increasing transport air velocity		0%	0-16%
Primary air partly replaced by steam, N ₂ or Ar		0%	Not tested
Addition of water sprays around burner		0%	Not tested
Addition of water to the secondary air		0%	Not tested
Switching to gas		≈ -250% [†]	Not tested
Switching to oil		≈ -250% [†]	25%***

* resulted in pellet quality problems

** using the reference burner. Larger reduction were seen with other burners

*** Oil is only used during startup and when operation issues occurs, which results in a high uncertainty of this value

[†] i.e. an increase in NO_x emission

5 Experimental equipment

This section describes the experimental facilities that are the basis of Paper I, as well as the measuring equipment used.

5.1 Experimental Combustion Facility

The experimental work in this thesis has been performed using LKAB's pilot-scale kiln, known as the Experimental Combustion Facility (ECF). In Year 2013, the heat input of the ECF was 400 kW_{fuel} but this was increased in Year 2015 to 580 kW_{fuel} and a cooling system was added to the bottom part of the kiln, to simulate the heat sink of pellets. Figure 5 is a schematic side-view of the Year 2015 ECF, which is the version that will be referred to hereinafter. The kiln is designed to replicate the combustion conditions in a full-scale rotary kiln. It is scaled down from approximately 40 MW_{fuel} with constant velocity scaling and has a diameter of 65 cm the first 4 meters. The length of the entire facility is 14 m, and after the first 4 m the diameter expands to 80 cm. The reason for extending the furnace is mainly to be able to perform e.g. slagging measurements. The rotation of the kiln, as well as the pellets is not included in the ECF. The ECF is equipped with both horizontally and vertically arranged access ports, which were used during the campaigns for in-flame measurements of temperature, concentrations, radiation, and heat flux. The temperature and concentration measurements in Paper I were obtained at four measurement ports (MH0, MH1, MH3 and MH7).

Hot secondary air enters through two channels located above and below the centrally positioned burner (through which the primary air and fuel are introduced). The burner is shown in Figure 6 and has six registers: two for primary air, and four for fuel. One primary air register is swirled (N4), while the other register introduces air axially (N1). Different fuel registers may be used depending on which full-scale plant the ECF simulates. In Paper I, the central fuel register (N6) was the most frequently used, although when co-combusting coal and biomass, coal was fed through N3 and biomass was fed through N2.

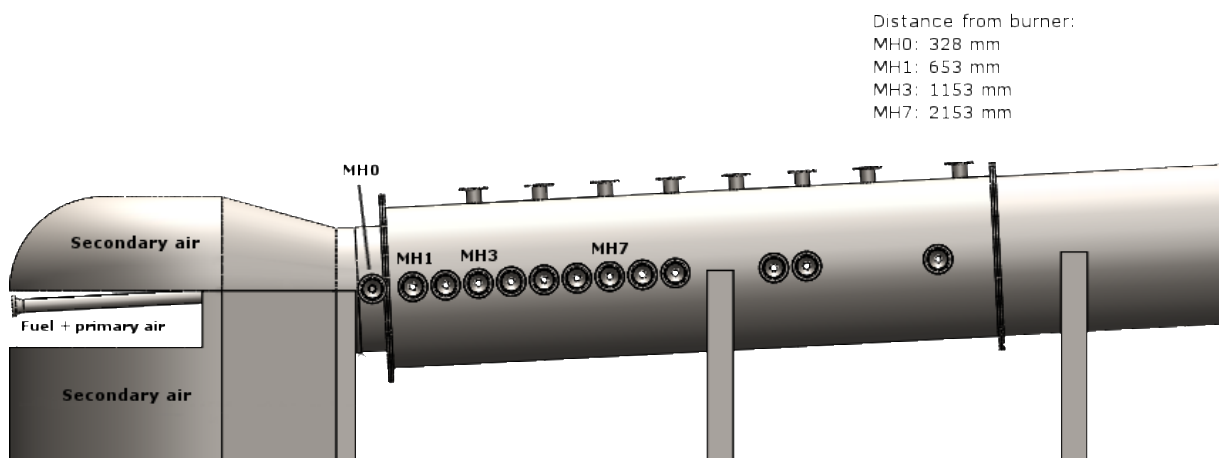


Figure 5. Side view of the ECF, showing the distances from the burner to the measurement ports. Source: Paper I

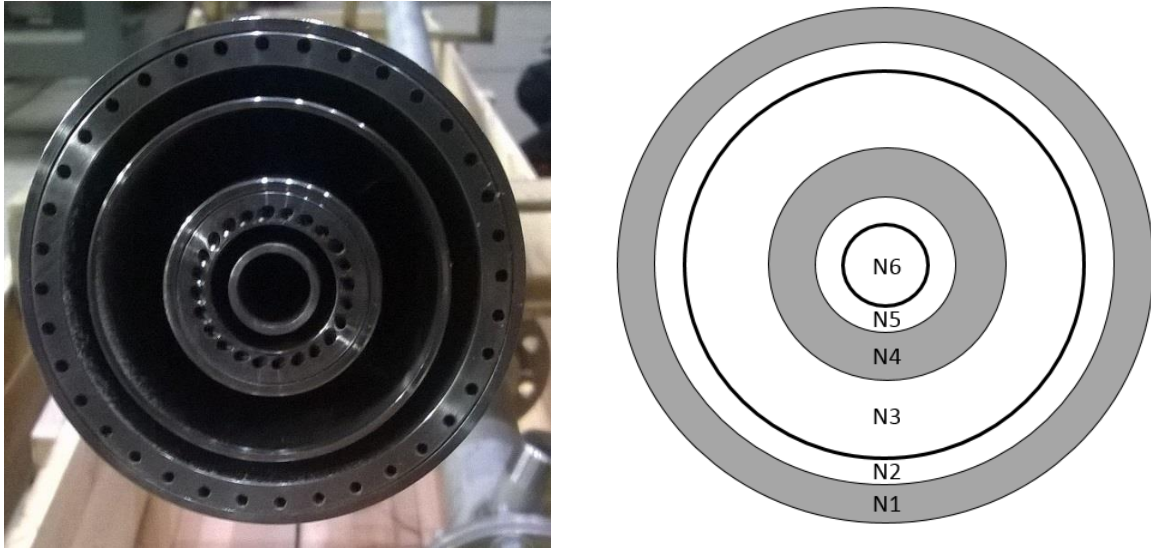


Figure 6. The burner orifice showing all six registers. Left: Photograph. Right: Schematic view with register annotations.

5.2 In-flame measurements

Performing in-flame measurements to map PF flames is challenging. Due to the turbulence of the flame, data are collected at each measurement position for a certain amount of time (several minutes) in order to get a representative average. Obtaining a good spatial resolution is thus time-consuming and difficult due to the unstable operating conditions disturbing the flame. Fluctuations in the fuel feed and processes that take a long time to stabilize, such as the wall temperatures (which may affect the flame), are parameters that are often difficult to keep stable.

Another challenge is to measure a property at a certain point with minimum disturbance of the flame. The most common forms of in-flame measurements are *intrusive*, i.e., a probe is inserted at the desired location and measures a property, either directly or by extracting gas or particles to be analyzed in external instrument. These probes need to be cooled due to the high flame temperatures, and the cooling itself affects the flame. The extent to which the flame is affected by the cooling is, however, difficult to establish. Ideally, one would want to perform measurements that are *non-intrusive*, which is becoming increasingly possible with the use of modern laser techniques. These are optical techniques that typically involve sending beams into the flame and measuring different occurrences with the use of detectors. Although there are many advantages and possibilities associated with such techniques, they usually require optical access at several sites, and it is not always clear how, for example, the laser beams affect the flame. Lasers themselves can also be large and require several fine adjustments, and it may be inconvenient to move them to, for example, another measurement port. Therefore, in terms of mobility and flexibility, intrusive measurements are more convenient to use. Nevertheless, there are optical measurement techniques that are portable and easy to use, e.g., IR cameras.

5.2.1 Temperature measurements

Temperature plays a central role in combustion and is an important parameter to measure if a comprehensive understanding of the flame is to be obtained. Measurements are performed with a thermocouple, which is a device that produces a temperature-dependent voltage from which

the temperature can be obtained. In theory, the thermocouple can be inserted directly into the flame and will be heated by convection to the temperature of the flame. Unfortunately, it is challenging to measure accurately, as the wall temperatures are lower than the flame temperatures and this causes a significant radiative cooling effect on the thermocouple, which results in a measurement error. This cooling effect can be reduced by shielding the thermocouple with a ceramic shell. The shielding also protects the thermocouple from physical damage by particles. Another measure that can be taken is to increase the convective heat transfer from the flame by applying suction around the thermocouple, which reduces the relative importance of the radiative loss. The gas velocity around the thermocouple should be around 200 m/s, so as to increase sufficiently the convective heat transfer. A drawback of applying suction is that the volume of gas that is sucked out of the flame makes the measurement less of a point measurement.

For the measurements performed in Paper I, a triple-shielded thermocouple of type B (suitable for $T < 1800^{\circ}\text{C}$) was mounted on a cooled probe with suction. The probe was then traversed across the flame. Even when the convective heat transfer was increased by suction, a waiting period of around 4 minutes was required for the thermocouple to stabilize at each measurement point. Figure 7 shows a schematic view of the suction pyrometer as well as a picture of the ceramic shield after an in-flame measurement.

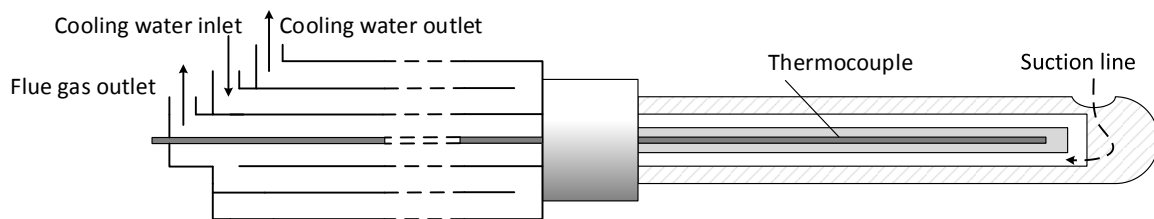


Figure 7. Top panel: Schematic of the probe showing how the thermocouple is protected by ceramics. Courtesy of Adrian Gunnarsson [69]. **Bottom panel:** Photograph of the protective ceramic around the thermocouple. The gas inlet is on the other side and is therefore not visible in this shot. Hot coal particles adhere to the ceramics after the measurements.

5.2.2 Gas composition measurements

There are several ways to measure the concentration of a specific gas in a gas mixture. A common approach is to force the gas mixture through a cell and direct light of a set wavelength, commonly infrared (IR) or ultraviolet (UV), through the cell towards a detector. If the gas mixture contains a gas that absorbs light of the set wavelength this will be detected by the detector and the attenuation of the light can be used to determine the actual concentration. A standard IR gas analyzer typically measures 1-3 gases simultaneously.

A technology that can effectively measure more gases simultaneously is Fourier Transform Infrared (FTIR) spectroscopy, which scans a wider range of wavelengths in the IR spectrum. Instead of using a light source that has only one wavelength (monochromatic), FTIR spectroscopy uses a light source with multiple wavelengths (polychromatic). The light from this source enters a so-called Michelson interferometer (Figure 8) where it encounters a beam splitter, which splits the beam into two beams, one of which is refracted to a fixed mirror and one of which is refracted to a moving mirror. The beams are reflected back to the beam splitter, where destructive and constructive interference occur depending on whether the wavelengths are in phase, which in turn is dependent upon the distances between the mirrors and the beam splitter. The resulting beam enters a sample cell that is filled with the gas mixture, where absorption of certain wavelengths occurs depending on the gases present in the mixture. The remaining beam is measured with a detector. Since one of the mirrors is moving, different distances between the mirror and beam splitter are achieved, and thus different wavelengths experience constructive/destructive interference, which means that the light entering the sample cell varies. The result is a so-called interferogram, which is transformed to a spectrum with the use of Fast Fourier Transform. A computer then compares this spectrum with a reference spectrum (typically an N₂ spectrum) and analyzes which wavelengths have been absorbed and to what extent. Knowing which wavelengths are relevant for which gases, it calculates the concentration of each gas. An issue with FTIR gas analyzers is that although every gas can be associated with a unique set of absorption wavelengths, a gas may share individual wavelengths with other gases, which may result in an error. For example, if gas A absorbs wavelengths x and y, which are also absorbed by gases B and C, it may appear that gas A is present even though only gases B and C are present. It is therefore necessary to have some idea as to which gases could be present. Another drawback is that FTIR spectrometers do not detect symmetrical diatomic gases (e.g., O₂), since these molecules lack a dipole moment and, therefore, will not interact with the electric field of the light. In the case of O₂ measurements, it is possible to use a paramagnetic instrument that relies on the magnetic property of O₂.

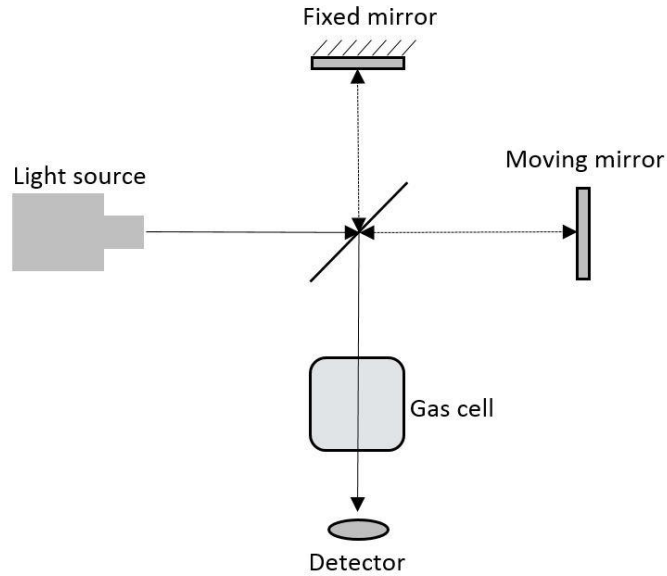


Figure 8. Schematic view of the Michelson interferometer which is central in FTIR spectroscopy.

For the gas concentration measurements performed in Paper I, the in-flame gases were extracted by suction and analyzed using FTIR spectroscopy and paramagnetism. The gas was suctioned through a filter, to protect the measurement equipment from particles, and was lead through an electrically heated tube ($\approx 190^{\circ}\text{C}$) to avoid condensation. The gas was assumed to experience instantaneous quenching. A schematic of the probe tip is depicted in Figure 9. A potential problem with these measurements is clogging of the filter by particles, which may cause unwanted heterogeneous reactions when the gas is suctioned through the filter. This can also cause unwanted pressure drops in the measurement equipment. Figure 9 also shows a photograph of the probe tip before measurements.

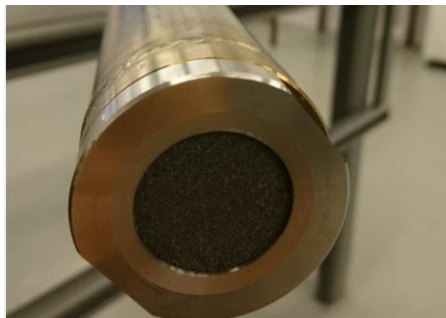
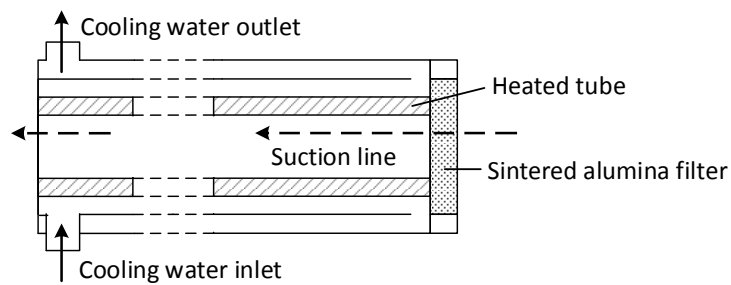


Figure 9. Top panel: Schematic side-view of the gas probe. Courtesy of Adrian Gunnarsson [69]. **Bottom panel:** Frontal view of the gas probe before any measurements.

6 Modeling

6.1 Overall modelling considerations

As described in the theory section, NO formation from solid fuel combustion is dependent on the pyrolysis process, volatile combustion and char combustion. The model developed in this work incorporates these processes to describe the NO formation, and the processes that relate to the combustion are treated as boundary conditions. Table 3 presents how the model treats the kinetics and the boundary conditions, such as mixing, heat release, heat transfer, species concentrations, temperature, and fuel characteristics, all of which all important and interconnected. The NO fractions that originate from vol-N and char-N are treated separately, and a major output from the model is the NO contribution from each of these two sources. Tars are not included in the model, and the pyrolysis process is assumed to be instantaneous. In the case of an iron ore rotary kiln, there could be interactions between the pellets and the combustion, e.g., thermal radiation and catalytic reactions. Such effects are however not included in the current model.

Table 3. Summary of ways in which combustion characteristics are treated in the modeling.

Combustion characteristic(s)	Treatment in the modeling
Kinetics	<ul style="list-style-type: none"> Detailed homogeneous reaction kinetics are used for the volatiles Apparent kinetics are used for the heterogeneous kinetics
Mixing	<ul style="list-style-type: none"> Mixing is defined by how fast air is added to the fuel in the axial direction Mixing on smaller scale (e.g., eddies and vortexes) is not considered
Heat release, heat transfer, and temperature	<ul style="list-style-type: none"> The energy equation is not solved. Instead, the temperature profile is given as an input from the measurements (or CFD)
Fuel composition	<ul style="list-style-type: none"> The volatiles are assumed to consist of CH₄, CO, H₂ and HCN Char and Char-N are modeled as C₂(s) and N₂(s) only converted through irreversible heterogeneous oxidation Ash is treated as a fully inert component Water is assumed to be in the form of vapor from the start
Particle characteristics	<ul style="list-style-type: none"> Properties related to the solid particles, such as porosity, surface area, fragmenting, and swelling, are neglected

6.2 Model description

The model describes the combustion chemistry and NO formation during combustion of a fuel. In theory, it could be used as a predictive model, although for this the model would require information on heat losses, to calculate the temperature profile, as well as an estimation of the mixing of the fuel and oxidizer, since the momentum equation is not included. Instead, providing the model with a temperature profile (from, for example, measurements) and fitting

the mixing profile to existing O₂ and CO concentrations avoids these uncertainties and provides a detailed description of the combustion conditions in a given process. Analysis of the reaction pathways and the governing reaction mechanisms may then be performed. Figure 10 presents a schematic overview of the model.

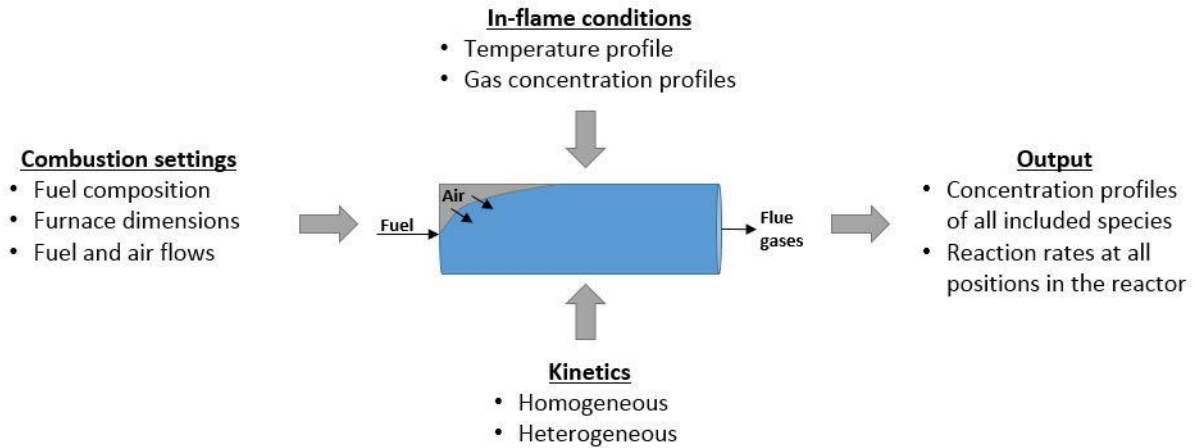


Figure 10. Illustration of the model structure with the inputs and outputs.

6.2.1 Mixing and kinetics

The in-flame combustion chemistry is modelled using a plug flow reactor (PFR) description, and mixing is described using a Zwietering approach [70]. The fuel is added at the main inlet to the PFR and the air is introduced in a staged manner. The staged insertion of air represents the mixing of the fuel and air. The air is divided into primary air and secondary air, with the primary air being injected more rapidly. The mixing rate is dependent upon the total flow of air and the share of the flow introduced at a given distance in the PFR (defined by the user). Mixing occurs rapidly if most of the air has been inserted at a short distance. The combustion chemistry is described by the detailed reaction kinetics proposed by Mendiara and Glarborg [71] for the homogeneous reactions, and the apparent kinetics are described by Jensen [72] for the heterogeneous reactions. The detailed homogeneous reaction mechanism involves 97 species and 779 reactions. In addition, three heterogeneous reactions with apparent kinetics are included: (i) the conversion of char into CO (R1); (ii) the oxidation of char-N to NO (R2); and (iii) the reduction of NO by char (R3&R4). The reduction of NO by char is described by two reactions in order to fit Chemkin's reaction arrangement. Table 4 presents the reactions and the corresponding kinetics. The mechanism assumes full conversion of char-N to NO. Thus, the reduction of NO by char, which depends on the local conditions, describes the apparent conversion.

Table 4. Reactions and kinetics of the heterogeneous mechanism.

Reaction	A [cm ³ /mol/s]	E _a [cal/mol]
R1 C ₂ (s) + O ₂ (g) -> 2 CO (g)	2.24E11	29,400
R2 N ₂ (s) + O ₂ (g) -> 2 NO (g)	2.24E11	29,400
R3 NO(g) + C ₂ (s) -> CO(g) + CN(s)*	1.46E11	29,400
R4 2 CN(s) -> C ₂ (s) + N ₂ (g)*	1.00E20	0

*The overall reaction $\text{NO}(\text{g}) + \frac{1}{2} \text{C}_2(\text{s}) \rightarrow \frac{1}{2} \text{N}_2(\text{g}) + \text{CO}(\text{g})$ is implemented as a two-step reaction, with R3 as the controlling step.

6.2.2 Fuel properties

The contents of volatiles, moisture, and ash, as well as the elemental composition of the fuel are given as inputs to the model. Moisture in the fuel is modeled as water vapor, i.e., the impact of vaporization is not included, and the ash is modeled as an inert component that does not interact with the combustion process. The char is represented as $C_2(s)$, and the volatiles are assumed to consist of CH_4 , H_2 , and CO . The split between the volatile components is determined by the elemental balances for C, H, and O:

$$Y_{CO} \left(\frac{M_C}{M_{CO}} \right) + Y_{CH_4} \left(\frac{M_C}{M_{CH_4}} \right) = \frac{X_{C,fuel} - X_{char}}{1 - X_{char}} \quad \text{Eq. 3}$$

$$Y_{H_2} \left(\frac{2M_H}{M_{H_2}} \right) + Y_{CH_4} \left(\frac{4M_H}{M_{CH_4}} \right) = \frac{X_{H,fuel}}{1 - X_{char}} \quad \text{Eq. 4}$$

$$Y_{CO} \left(\frac{M_O}{M_{CO}} \right) = \frac{X_{O,fuel}}{1 - X_{char}} \quad \text{Eq. 5}$$

where Y_i is the mass fraction of species i in the volatiles, M_j is the molar mass of element j , and X_k is the fuel mass fraction of element k in the fuel (dry, ash-free basis). The system of equations is then solved to obtain Y for CH_4 , H_2 , and CO . This approach is a simplification of the approach suggested by Thunman et al [73].

The nitrogen content of the fuel is split between the volatiles and char, i.e., a certain share is released with the volatiles as HCN , while the remainder is released with the char as $N_2(s)$. Assuming that the share is 50/50 and using Eqs. 3-5, the composition of a modeled fuel is obtained, as shown in Table 5 compared to the coal that it represents.

Table 5. Fuel composition of a coal used in the pilot-scale kiln [74] (Coal A) and the corresponding modeled fuel composition. The percentages are given on a wet basis.

Actual composition			Modeled composition		
Fixed carbon*	mass-%	64.6	$C_2(s)$	mass-%	63.9
Ash	mass-%	13.1	Ash	mass-%	13.1
H_2O	mass-%	0.9	$H_2O(g)$	mass-%	0.9
Volatile	mass-%	21.4	$CO(g)$	mass-%	8.2
C	mass-%	75.4	$CH_4(g)$	mass-%	11.1
H	mass-%	3.9	$H_2(g)$	mass-%	0.79
O	mass-%	5.9	$HCN(g)$	mass-%	1.32
N	mass-%	1.37	$N_2(s)$	mass-%	0.68
O_2-demand	m^3_n/kg_{fuel}	1.59	O_2-demand	m^3_n/kg_{fuel}	1.58

*Calculated by difference (100-Volatiles-Ash- H_2O).

6.2.3 Reaction analysis

The Chemkin solver calculates the rates of all reactions at each step in the PFR using the law of mass action:

$$rate = k \prod c_i^{v_i} \quad \text{Eq. 6}$$

where k is the rate constant (see Eq. 1), c_i is the i^{th} reactant in the reaction, and v_i is the stoichiometric coefficient for the i^{th} reactant. Reverse reactions are calculated with the use of thermodynamic data. The resulting rate at each step in the PFR is in mole/cm³/s. Since the purpose of the model is to evaluate NO formation under combustion, each rate has to be integrated in order to evaluate its overall importance. This can be done either over volume or residence time, depending on the desired outcome. The net formation of NO (in mol/s) in the PFR is obtained by integrating the net NO formation rate over the volume of the reactor. Likewise, the level of NO production from char-N and the level of NO reduction by char are calculated by integrating R2 and R3, respectively. The thermal NO formation is usually described by reactions R3-2 - R3-4 but due to the fact that the reverse reaction of R3-2 and the forward reaction of R3-4 are central to the net conversion of vol-N to NO, these reactions cannot simply be integrated to obtain the thermal NO formation. Instead, only the forward reactions of R3-2 and R3-3 are considered to be part of the thermal NO formation mechanism. Although it is possible to integrate the remainder of the homogeneous NO reactions to obtain a value for NO formation from vol-N, it becomes slightly misleading due to circular reactions (such as NO→HONO→NO₂→NO), which make volatile formation and reduction reactions appear more prominent than they actually are. Instead, the net amount of NO formed from the volatiles is calculated as the difference between the total net NO formation and the net level of NO formation from the processes of char-N formation, thermal NO formation, and NO reduction by char. In order to compare NO formation between combustion of different scale, the NO formation is divided by the fuel input (in MW_{fuel}). The resulting value is then in units of mol/MJ. Furthermore, since combustion processes use different fuels with different contents of nitrogen, this unit is in turn divided by the nitrogen content of the fuel (kg_N/kg_{fuel}). The final unit is displayed as mol/MJ/N, where N stands for the nitrogen content.

7 Results and discussion

The results are presented in two parts. First, the impacts on NO_x emission levels of the fuel and combustion parameters, based on the inputs and outputs of the ECF from the experimental campaign in Paper I, are presented. Previous results from a measurement campaign conducted in Year 2013 are also included. Second, the experimental results are evaluated through modeling, and the contributions of different formation mechanisms are analyzed. The evaluation concludes regarding the governing chemistry and the contribution from thermal NO, as well as regarding the conversion of vol-N and char-N.

7.1 NO_x performance

Figure 11 presents the levels of NO_x emissions detected in the ECF for the fuels tested in the Year 2013 and Year 2015 campaigns. The reference coal (Coal A) had approximately the same levels of NO_x emission in the two campaigns when the burner conditions were similar. Natural gas and oil produced significantly more NO_x than did the solid fuels, which is in agreement with previous work on rotary kilns [63-65]. Furthermore, the NO_x emissions from the solid fuels were high compared to those from conventional combustion – they reached levels that were 3-times the NO_x limit in the MCPD (shown in Figure 11). In both campaigns, Coal A produced the lowest amount of NO_x amongst the coals tested. Co-firing coal with biomass slightly reduced the level of NO_x compared to burning only Coal A (under similar combustion conditions). In the Year 2015 campaign, it was also shown that reducing the amount of primary air reduced the NO_x emissions significantly, and that even lower levels of NO_x were reached for Coal A (albeit still remarkably high), as compared to when co-firing was employed. Even though the levels of emissions were high, the solid fuels contained enough nitrogen to account for the emitted NO_x, and thermal NO did not necessarily predominate, as is usually assumed. Figure 12 presents the NO_x emissions and the ratio of outlet NO_x to inlet fuel-N flow (on a molar basis) as functions of the nitrogen contents of the solid fuels. The ratio varied between 0.8 and 0.4. A lower level of conversion to NO was obtained for fuels with a high content of nitrogen, even though the absolute level of NO_x emissions increased with nitrogen content. The trend that higher N-content leads to a lower ratio of outgoing NO_x to ingoing fuel-N has been observed in earlier studies of combustion [75].

In the Year 2015 campaign, the secondary air temperature varied within the range of 965°-1020°C, the outlet gas temperature varied within the range of 1200°-1300°C and the in-flame measurements yielded peak temperatures in the range of 1300°-1675°C (solid fuels only). The upper end of the range of the measured peak temperatures is clearly sufficiently high for thermal NO to be significant in terms of the kinetic rate constant, although the residence times at these temperatures, as well as the gas concentrations (e.g., N₂, O, and NO) are also crucial parameters. Figure 13 presents the NO_x emissions plotted against the measured peak temperature. Due to the low number of data-points, and the fact that the fuels vary in terms of nitrogen content, it is not possible to draw any definite conclusions from the figure. However, the spread seen in the figure (at least for ECF 2015) is an indication that thermal NO may not be dominating. Coal A was used in four experiments and appeared to produce less NO_x when higher peak temperatures

were measured. A similar observation in the Year 2015 campaign was that increasing the temperature of the secondary air decreased slightly the outgoing NO_x emissions. NO_x emissions are also clearly related to the nitrogen content of the fuel, which indicates the importance of fuel NO rather than thermal NO. Furthermore, it is known that increasing the air-to-fuel ratio increase fuel-N conversion, and even though there is a shortage of data for the high air-to-fuel ratio used in iron ore rotary kilns, similar conversion values have been reported (see for example Pohl et al [25]). These facts point towards high fuel-N conversion being important, rather than high thermal NO formation.

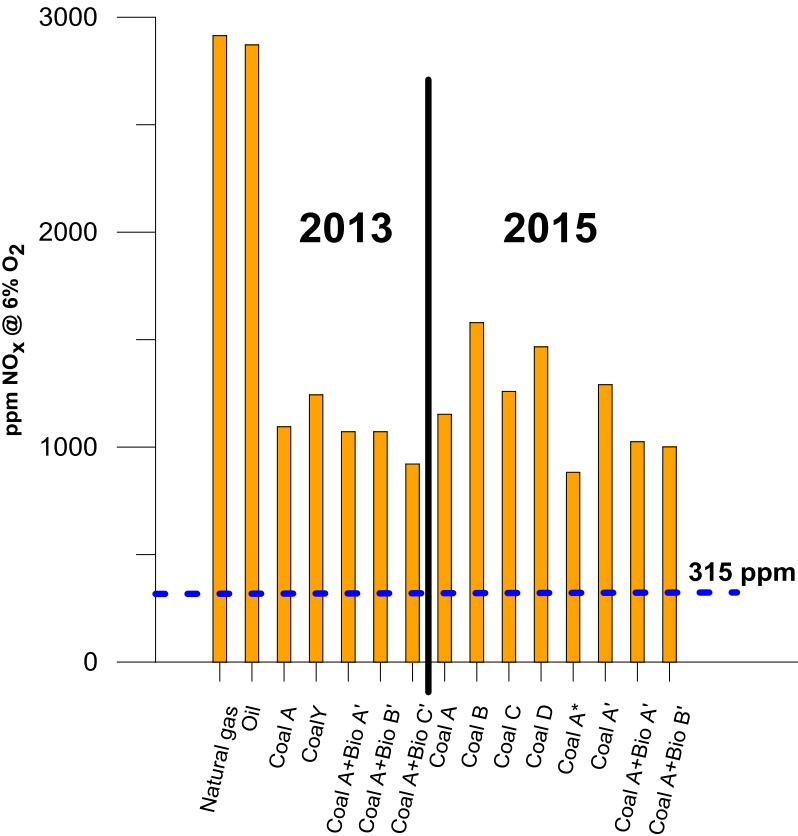


Figure 11. NO_x emissions for the fuels tested during the Year 2013 and Year 2015 campaigns. Coal A is the reference coal, which is used at full scale. *, Lower amount of primary air. ', Different burner configuration (not the same in years 2013 and 2015). Blue dashed line: the MCPD limit.

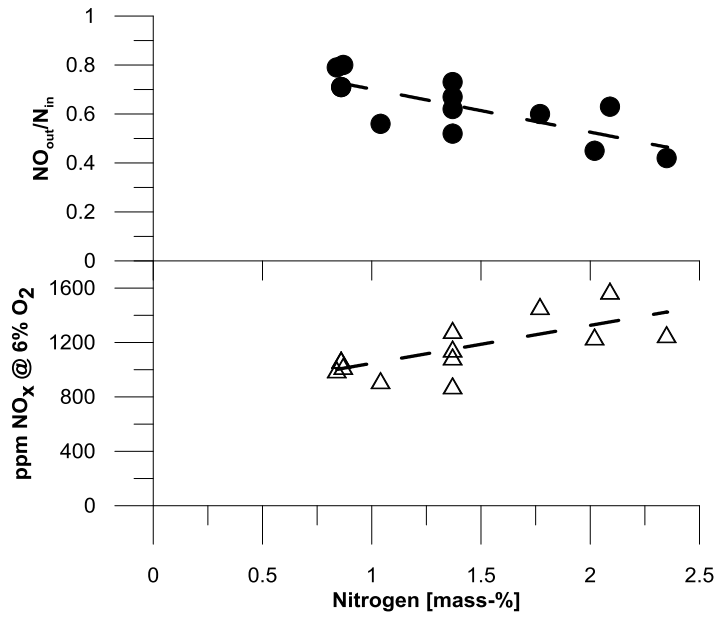


Figure 12. Levels of NO_x emissions and the ratios of outlet NO to inlet N (on a molar basis) as functions of the nitrogen content of the fuel.

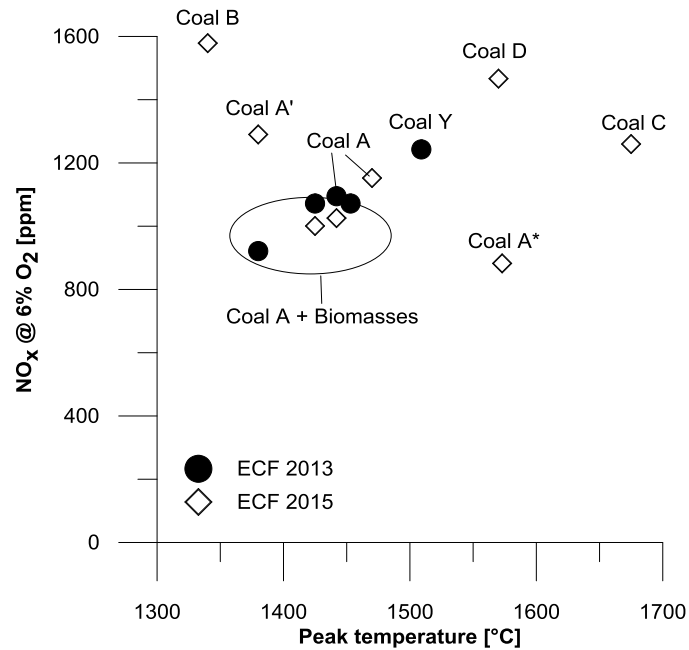


Figure 13. NO_x emissions compared to measured peak temperature for both measurement campaigns.

7.2 Contributions of thermal NO and fuel NO formation mechanisms

In order to propose measures for NO_x reduction in iron ore rotary kilns, it is important to estimate the different contributions of the NO-forming mechanisms. This is especially interesting because the experimental results indicate that the general assumption – that thermal NO formation predominates in iron ore rotary kilns – may not be valid. There is, however, not a clear cut between the contributions of thermal NO and fuel NO to total NO_x formation, since

the respective formation mechanisms are not completely exclusive. The main connection between the two mechanisms is reaction R 3-2, since the forward reaction is the rate-limiting step for the thermal reaction, while the reverse reaction is the main reaction for homogeneous reduction of NO, which is central to the chemistry governing the conversion of vol-N.

As mentioned, lower levels of primary air resulted in lower levels of NO_x emissions in the campaign conducted in Year 2015. Figure 14 presents the temperature profiles for the two cases with different levels of primary air (Coal A and Coal A* in Figure 11), as obtained by both suction pyrometry and the use of an IR-camera. As can be seen, the temperatures are significantly higher when low levels of primary air are used. Figure 15 presents the center line in-flame measurements of NO and O₂, together with the fitted model described in Section 6.2. Significantly lower concentrations of O₂ were measured early on in the case with low levels of primary air (Coal A*), which indicates the presence of a pronounced reducing zone. Therefore, a reduction in the conversion of vol-N to NO is thought to be the reason for the lower level of NO_x emissions.

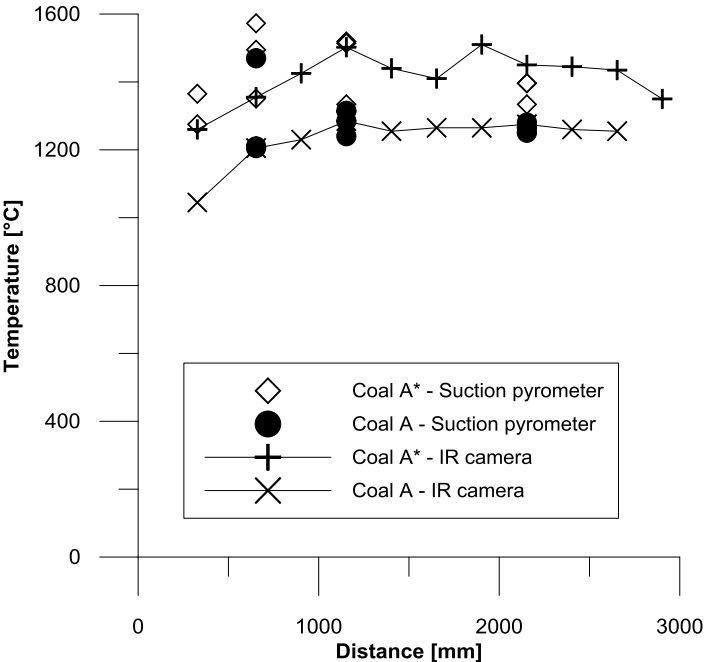


Figure 14. Measured temperature profiles for a case with a low level of primary air (Coal A*) and a case with a high level of primary air (Coal A). The temperatures were obtained with both a suction pyrometer and an IR-camera. For the suction pyrometer measurements, only the three centre-line measurements are included.

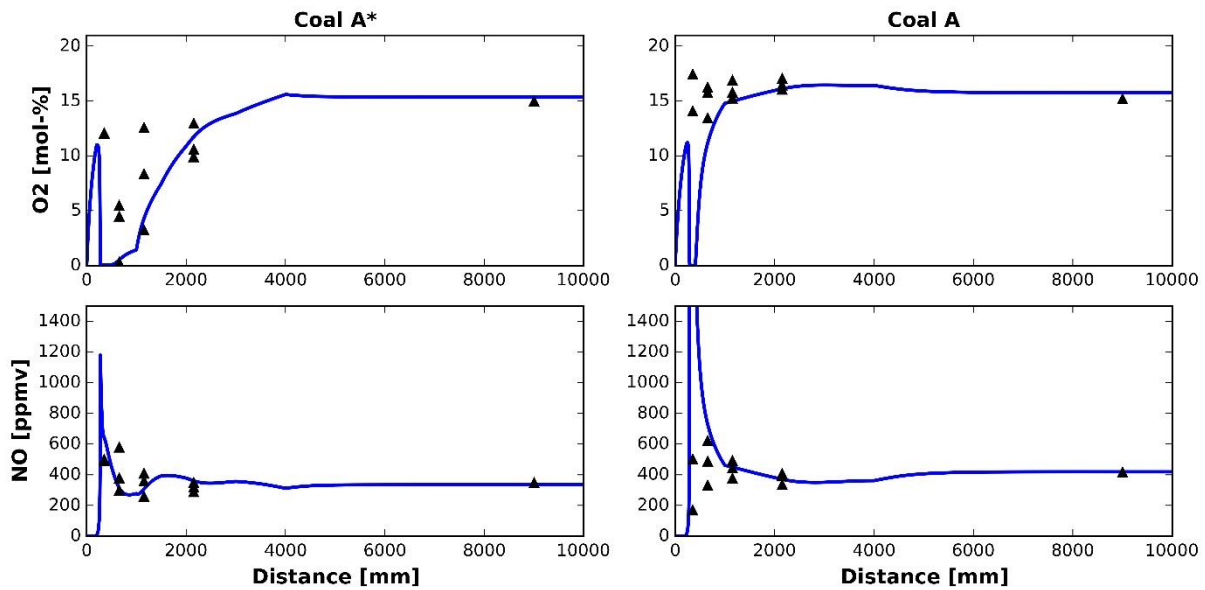


Figure 15. In-flame measurements of O_2 and NO for a case with a low level of primary air (Coal A*) and a case with a high level of primary air (Coal A). The O_2 concentrations are shown on a dry basis, and the NO concentrations on a wet basis. Symbols: Measurements. Line: Model. Source: Paper II.

In Paper II, modeling was used to evaluate Coal A and Coal A*. As a reference point, the model was also applied to previous measurements carried out in a 100-kW_{fuel} facility that combusted lignite [76]. This case will be referred to as ‘Lignite’. Figure 16 presents a comparison of the gas profiles of O_2 , NO, CO, and CO_2 after fitting the model to the experiments. Since the lengths of the two combustion facilities are different, the x-axis in Figure 16 is normalized. The combustion process can be assumed to be complete when the concentrations have stabilized. Figure 17 presents the resulting levels of NO formation/reduction. Three main conclusions are drawn from Figure 17:

- Thermal NO appears to be negligible
- The increased conversion of vol-N to NO is responsible for the higher formation of NO_x seen for Coal A, as compared to Coal A*
- The level of NO reduction by char is low in rotary kilns, as compared to the corresponding level in the 100-kW combustor, i.e., apparent char-N conversion is high in rotary kilns and is responsible for the high levels of NO_x emissions

The first and second points are in accordance with the indications from the experimental results. The third point constitutes perhaps the main conclusion of this thesis: high apparent conversion of char-N is the main reason for the high levels of NO_x emissions in iron ore rotary kilns. Since the intrinsic rate of char-N conversion to NO is modelled as 100%, the reduction of NO by char is the governing mechanism. The reduction reaction (R3) requires both NO and char, so high concentrations of these components are beneficial. However, the high air-to-fuel ratio employed in iron ore rotary kilns counteract this, since both components are diluted by the large gas flow, and the high concentration of O_2 in the burnout zone (i.e., after volatile combustion) leads to rapid consumption of char. With the used kinetics, the ratio of the NO reduction rate (R2) to the rate of char consumption by O_2 (R1) gives an indication of the effectiveness of the NO reduction mechanism. The ratio between these rates becomes:

$$\frac{R_3}{R_1} = \frac{A_3 [NO]}{A_1 [O_2]} \quad \text{Eq. 7}$$

An increased ratio of NO to O₂ indicates that the char may reduce a larger amount of NO before being consumed by O₂. As can be seen in Figure 16, the O₂ levels are significantly higher in the rotary kiln cases, while the NO levels are similar. The result is low NO reduction by char.

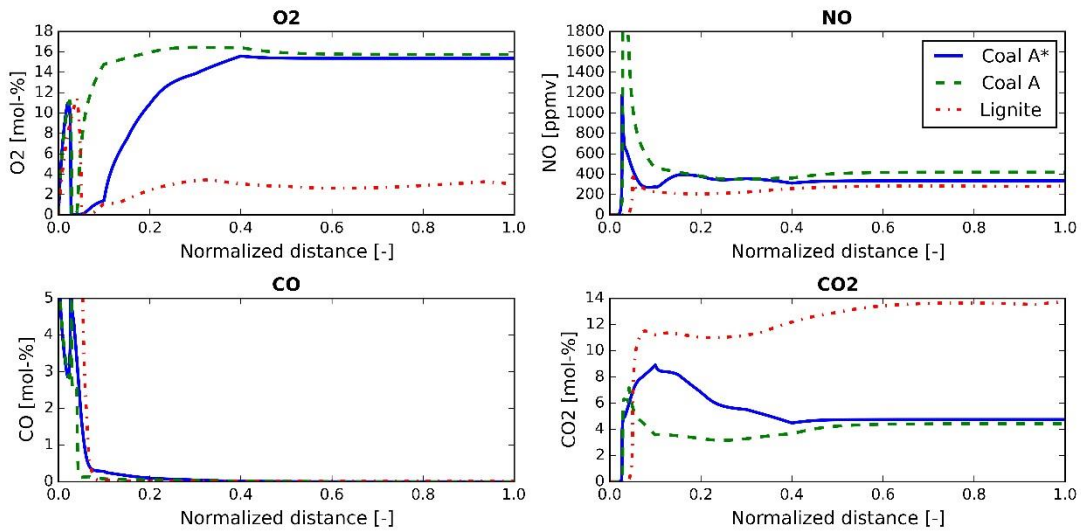


Figure 16. Gas profiles derived in the model for the three cases. Coal A* and Coal A are based on the ECF Year 2015 cases shown in Figure 11. The Lignite case was not performed in a rotary kiln. Source: Paper II

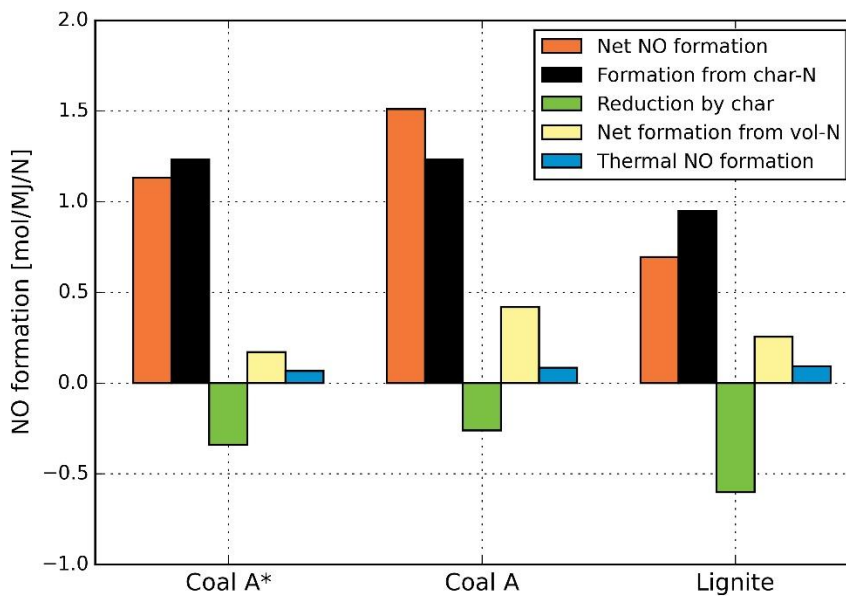


Figure 17. Calculated formation/reduction contributions for the three cases. Coal A* and Coal A are based on the ECF Year 2015 cases shown in Figure 11. The Lignite experiment was not performed in a rotary kiln. Source: Paper II

As char combustion occurs further away from the burner than volatiles combustion, it is less dependent upon the burner design. Modifying the air-to-fuel ratio is one way to increase the NO/O₂ ratio after volatile combustion, thereby influencing the conversion of char-N. However,

drastically reducing λ from 4.2 to 2.8 (brought about by reducing the oxygen content in the secondary “air”, while keeping the same volumetric flow), as tested in an experiment (Paper I), decreased the conversion to NO ($\text{NO}_{\text{out}}/\text{N}_{\text{in}}$) from 0.67 to 0.59, which is a rather small reduction. This is also not a particularly attractive measure to apply in full-scale kilns, since the partial pressure of O_2 is important for pellet quality.

A possible measure to reduce the ratio of O_2 to NO without reducing the amount of excess air is to recirculate the flue gases. However, achieving significant reductions in the O_2 concentrations would require high levels of gas recirculation due to the high levels of O_2 post-combustion (15%-16% without recirculation). An alternative approach is to enhance the combustion through oxygen addition, thereby achieving the level of oxygen required for combustion and pellet oxidation while reducing the dilution effect of NO (since less N_2 is added). This latter approach is briefly evaluated in Paper II and appears to have potential, although it is unclear how the temperature profile would be affected.

The second bullet point obtained from Figure 17 is simply a consequence of the amount of available oxygen during vol-N conversion. This is controlled by the mixing rate of air to the fuel, as well as the point of fuel ignition. The latter is strongly temperature-dependent, and achieving a high initial temperature is beneficial for rapid ignition. In Paper III, an investigation of the homogenous chemistry during volatiles combustion was performed by setting up an isothermal PFR with a fuel inlet that consisted of CH_4 and HCN, with a staged insertion of air. The total residence time was set to 1 s, independent of the conditions used. Figure 18 presents the ratio of outgoing NO to ingoing vol-N as functions of temperature and mixing rate (described as the time that elapses until mixing is complete). At low temperatures ($<1000^\circ\text{C}$), the ratio is low due to incomplete combustion, which leads to a low rate of conversion of vol-N. At high temperatures ($>1600^\circ\text{C}$), the ratio is greater than unity due to the onset of thermal NO formation. Between these regimes, vol-N conversion exhibits a step change that is dependent upon the mixing rate and temperature. This characterizes a shift from transport-controlled to kinetics-controlled conversion. A case in which the mixing is rapid and the temperature is low leads to significantly higher vol-N conversion than a case in which the temperature is high (but $<1600^\circ\text{C}$) and mixing is slow. In other words, if the addition of oxygen through mixing is faster than the consumption of oxygen by reactions, NO formation increases significantly. Figure 19 presents a reaction pathway analysis for a transport-controlled case and a kinetics-controlled case. Only the most important species and reaction pathways are shown. The main difference between the cases is that the formation of NO from NCO and NH is important in the kinetically controlled case, while in the mixing-controlled case, NO is mainly produced by the reaction between the N-radical and OH. In addition, in the kinetically controlled case, the reduction of NO by the N-radical is negligible.

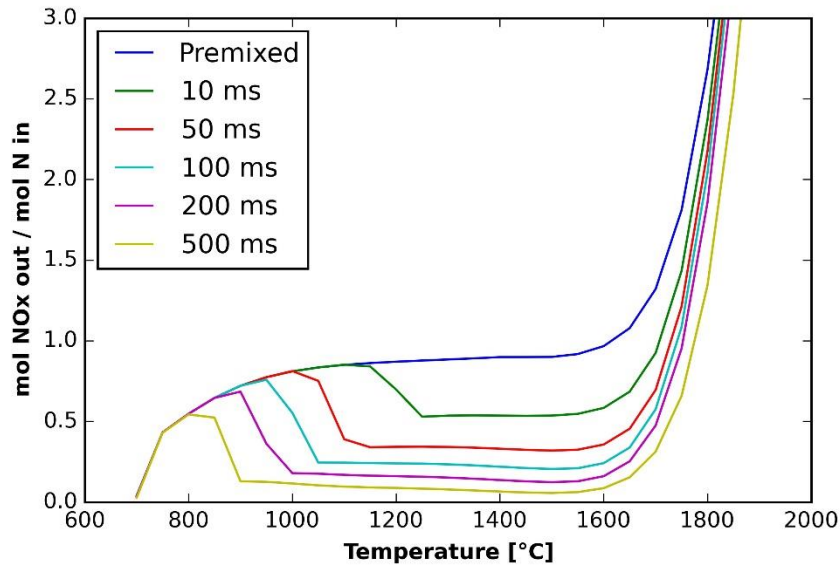


Figure 18. Ratio of outgoing NO_x to ingoing vol-N as a function of temperature and mixing time (equivalent to the mixing rate). Based on Paper III.

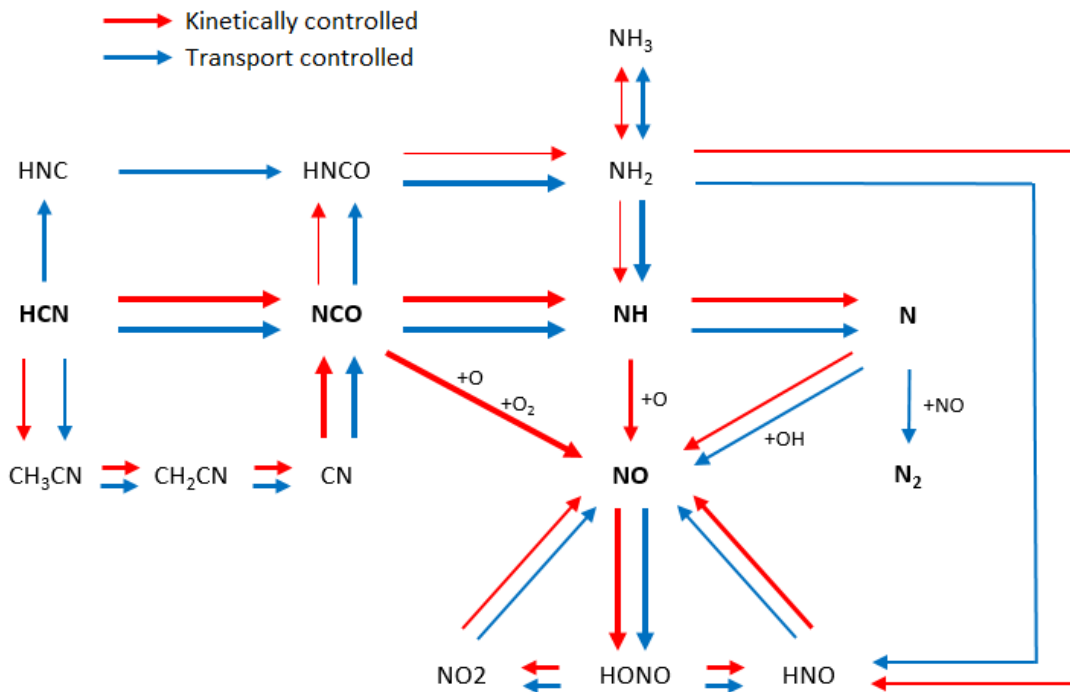


Figure 19. Reaction analysis of a kinetically controlled case and a transport-controlled case. The thickness of each line indicates the relative importance of that reaction step. Source: Paper III

Since char-N conversion may be difficult to control without reducing the equivalence air-to-fuel ratio close to unity, and since vol-N conversion can be reduced through burner staging, measures to control the fuel-N that is released with the volatiles rather than the char might represent the best alternative amongst the primary measures. In theory, this could be achieved by increasing the pyrolysis temperature. However, a prerequisite for this is a better description of the pyrolysis process than we have in the current model, and the practical feasibility of this has to be evaluated in further studies.

8 Summary

This thesis presents an investigation of the formation of NO_x in iron ore rotary kilns that combust solid fuels. The impact of changing to alternative coals, as well as that of co-combusting coal and biomass were investigated. The effects of changing combustion settings were also examined. The research involved experiments in a pilot-scale kiln ($580\text{kW}_{\text{fuel}}$), combined with modeling work that focused on the combustion chemistry.

The experimental investigation shows that the amount of primary air has a significant impact on NO_x emissions. A case with a low level of primary air emitted significantly less NO_x than a case in which the level of primary air was high. In-flame measurements revealed that the temperature was actually higher in the case with a low level of primary air, even though amount of NO_x formation was reduced. The measurements also revealed the presence of an O_2 -lean zone in front of the burner when the level of primary air was low. This zone was absent in the case with a higher level of primary air. The main reason for the reduction in NO_x formation is thought to be decreased conversion of vol-N to NO. Other measures that reduced NO_x emissions included the co-combustion of coal and biomass, reducing the air-to-fuel ratio, and increasing the secondary air temperature.

The results from the modeling confirm that the conversion of vol-N to NO is significantly increased when an O_2 -lean zone is absent. The reaction analysis shows that under highly oxidizing conditions, vol-N conversion becomes kinetically controlled rather than transport-controlled, which promotes significant NO formations. When comparing the contributions of char-N and vol-N to the total NO formation under iron ore rotary kiln conditions to that employed in more conventional combustion, it is clear that the apparent conversion of char-N to NO is significantly higher in the rotary kiln. This high level of conversion is attributed to a high O_2/NO ratio, which promotes an oxidizing environment and a low efficiency of NO reduction by char. Furthermore, thermal NO formation appears to be negligible in all investigated cases.

Given the difficulties associated with controlling the conversion of char-N to NO, plans to create conditions in which the fuel-N is released with the volatiles rather than the char appear to be an avenue for future research.

9 Future work

The results from the modeling work indicate that exploring the possibility of increasing the fraction of nitrogen released with the volatiles might be a solution for reducing NO_x formation in iron ore rotary kilns. A detailed investigation of the pyrolysis process would thus be a logical continuation of this thesis. There exist available pyrolysis models with the inclusion of nitrogen species on the web, which might be a first step. Furthermore, since the results indicate that the solid-gas reactions are of utmost importance, the model needs to cover this in more detail. In particular, the importance of mass transfer has to be evaluated and ways to describe the process when mass transfer is limiting the combustion process. Some kind of particle model could be developed to complement the current model.

Apart from investigating the pyrolysis process further, there are three experimental paths forward. The first is to perform more experiments in LKABs pilot kiln, similar to those that Paper I and Paper II are based on. More focus on burner settings as well as modifications of the secondary air would be interesting from a NO_x perspective. The second possibility is to attempt to apply the lessons learned from the pilot scale to full scale. A problem encountered in previous attempts to reduce NO_x is that the results from the pilot kiln did not transfer to the full scale kiln, and it would be interesting to see if the new modifications to the pilot kiln changes this.

Apart from an environmental and economic perspective, there is thus also a scientific desire for more research on the NO formation in iron ore rotary kilns. The combustion of pulverized fuel at elevated temperatures and at higher-than-normal partial pressures of oxygen has received attention in recent years due to the development of oxy-fuel combustion, but the impact on NO formation when N_2 is present is not well documented. A path forward is to apply laser technology to measure e.g. OH radicals and soot concentrations. This can provide valuable information of the combustion chemistry and flame structure.

References

- [1] S. V. Krupa and W. J. Manning, "Atmospheric ozone: Formation and effects on vegetation," *Environmental Pollution*, vol. 50, pp. 101-137, 1988/01/01/ 1988.
- [2] J. Fuhrer, L. Skärby, and M. R. Ashmore, "Critical levels for ozone effects on vegetation in Europe," *Environmental Pollution*, vol. 97, pp. 91-106, 1997/01/01/ 1997.
- [3] W. H. Organization, "Health aspects of air pollution with particulate matter, ozone and nitrogen dioxide: report on a WHO working group, Bonn, Germany 13-15 January 2003," 2003.
- [4] J. Rose, *Acid rain: current situation and remedies* vol. 4. Yverdon: Gordon and Breach, 1994.
- [5] C. Price, J. Penner, and M. Prather, "NO_x from lightning: 1. Global distribution based on lightning physics," *Journal of Geophysical Research: Atmospheres*, vol. 102, pp. 5929-5941, 1997.
- [6] R. Zhang, X. Tie, and D. W. Bond, "Impacts of anthropogenic and natural NO_x sources over the US on tropospheric chemistry," *Proceedings of the National Academy of Sciences*, vol. 100, pp. 1505-1509, 2003.
- [7] UNECE. (2017-06-30). *Air Pollution*. Available: <http://www.unece.org/env/lrtap/welcome.html>
- [8] "1999 Protocol to Abate Acidification, Eutrophication and Ground-level Ozone to the Convention on Long-range Transboundary Air Pollution," ed: Gothenburg, 1999.
- [9] EU, "Directive (EU) 2016/2284 of the European Parliament and of the Council of 14 December 2016 on the reduction of national emissions of certain atmospheric pollutants," 2016.
- [10] CLRTAP. WebDab Search [Online]. Available: http://webdab1.umweltbundesamt.at/official_country_year.html?cgiproxy_skip=1
- [11] EU, "Directive 2010/75/EU of the European Parliament and of the Council of 24 November 2010 on industrial emissions (integrated pollution prevention and control) Text with EEA relevance," 2010.
- [12] EU, "Directive (EU) 2015/2193 of the European Parliament and of the Council of 25 November 2015 on the limitation of emissions of certain pollutants into the air from medium combustion plants (Text with EEA relevance)," 2015.
- [13] Naturvårdsverket. (2017-06-30). *Resultat för kväveoxidavgiften*. Available: <http://www.naturvardsverket.se/Miljoarbete-i-samhallet/Miljoarbete-i-Sverige/Uppdelat-efter-omrade/Energi/Kvaveoxidavgiften/Resultat-for-kvaveoxidavgiften/>
- [14] Naturvårdsverket, "Vägledning till NFS 2016:13 - för versamhetsutövare," 2017.
- [15] Naturvårdsverket, "Genomförande av MCP-direktivet," 2017.
- [16] JRC, "Best Available Techniques (BAT) Reference Document for Iron and Steel Production " 2010.
- [17] W. S. Association, "World Steel in Figures 2017," 2017.
- [18] U. G. Survey, "Global Iron Ore Production Data; Clarification of Reporting from the USGS," 2017.
- [19] U. S. G. Survey, "Mineral commodity summaries 2017," 2017.
- [20] D. Pershing and J. Wendt, "Pulverized coal combustion: The influence of flame temperature and coal composition on thermal and fuel NO_x," in *Symposium (International) on Combustion*, 1977, pp. 389-399.

- [21] Y. Zeldovich, D. Frank-Kamenetskii, and P. Sadovnikov, *Oxidation of nitrogen in combustion*: Publishing House of the Acad of Sciences of USSR, 1947.
- [22] P. Glarborg, "Fuel nitrogen conversion in solid fuel fired systems," *Progress in Energy and Combustion Science*, vol. 19, pp. 89-113, 2002.
- [23] H. Zhang and T. H. Fletcher, "Nitrogen transformations during secondary coal pyrolysis," *Energy & fuels*, vol. 15, pp. 1512-1522, 2001.
- [24] D. Blair, J. O. Wendt, and W. Bartok, "Evolution of nitrogen and other species during controlled pyrolysis of coal," in *Symposium (International) on Combustion*, 1977, pp. 475-489.
- [25] J. H. Pohl and A. F. Sarofim, "Devolatilization and oxidation of coal nitrogen," in *Symposium (International) on Combustion*, 1977, pp. 491-501.
- [26] P. R. Solomon and M. B. Colket, "Evolution of fuel nitrogen in coal devolatilization," *Fuel*, vol. 57, pp. 749-755, 1978.
- [27] S. Kambara, T. Takarada, Y. Yamamoto, and K. Kato, "Relation between functional forms of coal nitrogen and formation of nitrogen oxide (NO_x) precursors during rapid pyrolysis," *Energy & Fuels*, vol. 7, pp. 1013-1020, 1993.
- [28] P. R. Solomon, D. G. Hamblen, M. A. Serio, Z.-Z. Yu, and S. Charpenay, "A characterization method and model for predicting coal conversion behaviour," *Fuel*, vol. 72, pp. 469-488, 1993.
- [29] S. Niksa, "FLASHCHAIN theory for rapid coal devolatilization kinetics. 3. Modeling the behavior of various coals," *Energy & Fuels*, vol. 5, pp. 673-683, 1991.
- [30] T. H. Fletcher, A. R. Kerstein, R. J. Pugmire, M. Solum, and D. M. Grant, "A chemical percolation model for devolatilization: summary," *Brigham Young University*, 1992.
- [31] J. O. Wendt and C. Sternling, "Effect of ammonia in gaseous fuels on nitrogen oxide emissions," *Journal of the Air Pollution Control Association*, vol. 24, pp. 1055-1058, 1974.
- [32] J. A. Miller and C. T. Bowman, "Mechanism and modeling of nitrogen chemistry in combustion," *Progress in Energy and Combustion Science*, vol. 15, pp. 287-338, 1989/01/01 1989.
- [33] G. P. Smith, D. M. Golden, M. Frenklach, N. W. Moriarty, B. Eiteneer, M. Goldenberg, *et al.*, "GRI-Mech 3.0, 2000," URL http://www.me.berkeley.edu/gri_mech.
- [34] J. C. Chen and S. Niksa, "Suppressed nitrogen evolution from coal-derived soot and low-volatility coal chars," *Symposium (International) on Combustion*, vol. 24, pp. 1269-1276, 1992/01/01 1992.
- [35] G. J. Haussmann and C. H. Kruger, "Evolution and reaction of coal fuel nitrogen during rapid oxidative pyrolysis and combustion," *Symposium (International) on Combustion*, vol. 23, pp. 1265-1271, 1991/01/01 1991.
- [36] M. T. Cheng, M. J. Kirsch, and T. W. Lester, "Reaction of nitric oxide with bound carbon at flame temperatures," *Combustion and Flame*, vol. 77, pp. 213-217, 1989/08/01 1989.
- [37] M. Østberg, P. Glarborg, A. Jensen, J. E. Johnsson, L. S. Pedersen, and K. Dam-Johansen, "A model of the coal reburning process," *Symposium (International) on Combustion*, vol. 27, pp. 3027-3035, 1998/01/01 1998.
- [38] D. Phong-Anant, L. Wibberley, and T. Wall, "Nitrogen oxide formation from Australian coals," *Combustion and flame*, vol. 62, pp. 21-30, 1985.
- [39] Y. H. Song, J. H. Pohl, J. M. Beér, and A. F. Sarofim, "Nitric oxide formation during pulverized coal combustion," *Combustion science and technology*, vol. 28, pp. 31-40, 1982.

- [40] J. P. Spinti and D. W. Pershing, "The fate of char-N at pulverized coal conditions," *Combustion and Flame*, vol. 135, pp. 299-313, 2003.
- [41] D. Pershing and J. Wendt, "Relative contributions of volatile nitrogen and char nitrogen to NO_x emissions from pulverized coal flames," *Industrial & Engineering Chemistry Process Design and Development*, vol. 18, pp. 60-67, 1979.
- [42] A. Molina, E. G. Eddings, D. W. Pershing, and A. F. Sarofim, "Nitric oxide destruction during coal and char oxidation under pulverized-coal combustion conditions," *Combustion and Flame*, vol. 136, pp. 303-312, 2004.
- [43] P. F. Nelson, P. C. Nancarrow, J. Bus, and A. Prokopiuk, "Fractional conversion of char N to NO in an entrained flow reactor," *Proceedings of the Combustion Institute*, vol. 29, pp. 2267-2274, 2002.
- [44] L. S. Jensen, H. E. Jannerup, P. Glarborg, A. Jensen, and K. Dam-Johansen, "Experimental investigation of NO from pulverized char combustion," *Proceedings of the Combustion Institute*, vol. 28, pp. 2271-2278, 2000.
- [45] A. Molina, J. J. Murphy, F. Winter, B. S. Haynes, L. G. Blevins, and C. R. Shaddix, "Pathways for conversion of char nitrogen to nitric oxide during pulverized coal combustion," *Combustion and Flame*, vol. 156, pp. 574-587, 2009.
- [46] S. P. Visona and B. R. Stanmore, "Modeling NO_x release from a single coal particle II. Formation of NO from char-nitrogen," *Combustion and Flame*, vol. 106, pp. 207-218, 1996/08/01 1996.
- [47] T. Shimizu, Y. Sazawa, T. Adschiri, and T. Furusawa, "Conversion of char-bound nitrogen to nitric oxide during combustion," *Fuel*, vol. 71, pp. 361-365, 1992/04/01 1992.
- [48] W. Wang, S. D. Brown, C. J. Hindmarsh, and K. M. Thomas, "NO_x release and reactivity of chars from a wide range of coals during combustion," *Fuel*, vol. 73, pp. 1381-1388, 1994.
- [49] I. Glassman and R. A. Yetter, "Chapter 9 - Combustion of Nonvolatile Fuels," in *Combustion (Fourth Edition)*, ed Burlington: Academic Press, 2008, pp. 495-550.
- [50] R. H. Hurt and J. M. Calo, "Semi-global intrinsic kinetics for char combustion modeling," *Combustion and Flame*, vol. 125, pp. 1138-1149, 2001/05/01/ 2001.
- [51] R. Barranco, A. Rojas, J. Barraza, and E. Lester, "A new char combustion kinetic model 1. Formulation," *Fuel*, vol. 88, pp. 2335-2339, 2009/12/01/ 2009.
- [52] W. Chen, L. Smoot, S. Hill, and T. Fletcher, "Global rate expression for nitric oxide reburning. Part 2," *Energy & fuels*, vol. 10, pp. 1046-1052, 1996.
- [53] B. Coda, F. Kluger, D. Förtsch, H. Spliethoff, K. Hein, and L. Tognotti, "Coal-nitrogen release and NO_x evolution in air-staged combustion," *Energy & fuels*, vol. 12, pp. 1322-1327, 1998.
- [54] I. Aarna and E. M. Suuberg, "A review of the kinetics of the nitric oxide-carbon reaction," *Fuel*, vol. 76, pp. 475-491, 1997.
- [55] Y. H. Song, J. M. BEÉR, and A. F. SAROFIM, "Reduction of nitric oxide by coal char at temperatures of 1250–1750 K," 1981.
- [56] L. Chan, A. Sarofim, and J. Beer, "Kinetics of the NO • carbon reaction at fluidized bed combustor conditions," *Combustion and Flame*, vol. 52, pp. 37-45, 1983.
- [57] M. Sami, K. Annamalai, and M. Wooldridge, "Co-firing of coal and biomass fuel blends," *Progress in Energy and Combustion Science*, vol. 27, pp. 171-214, 2001/01/01/ 2001.
- [58] A.-K. Hjalmarsson, *NO_x control technologies for coal combustion: IEA Coal Research*, 1990.
- [59] C. Baukal and P. Eleazer, "Quantifying NO_x for industrial combustion processes," *Journal of the Air & Waste Management Association*, vol. 48, pp. 52-58, 1998.

- [60] A. A. Boateng, *Rotary kilns: transport phenomena and transport processes*: Butterworth-Heinemann, 2008.
- [61] M. H. Vaccaro, "Low NO_x rotary kiln burner technology: design principles & case study," in *Cement Industry Technical Conference, 2002. IEEE-IAS/PCA 44th*, 2002, pp. 265-270.
- [62] A. T. McQueen, S. J. Bortz, M. S. Hatch, and R. L. Leonard, "Cement kiln NO_x control," *IEEE transactions on industry applications*, vol. 31, pp. 36-44, 1995.
- [63] R. Battye, S. J. Walsh, J. Lee-Greco, and D. Sanders, *NO_x Control Technologies for the Cement Industry*: US Environmental Protection Agency, Office of Air Quality Planning and Standards, Air Quality Strategies and Standards Division, 2000.
- [64] F. Schorcht, I. Kourti, B. Scalet, S. Roudier, and L. Sancho, "Best Available Techniques (BAT), Reference Document for the Production of Cement, Lime and Magnesium Oxide: Industrial Emissions Directive 2010/75/EU:(Integrated Pollution Prevention and Control)," *JRC Reference Reports; Publications Office of the European Union*, 2013.
- [65] J. Bolen, "Modern air pollution control for iron ore induration," *Minerals & Metallurgical Processing*, vol. 31, 2014.
- [66] R. A. Davis, "Nitric oxide formation in an iron oxide pellet rotary kiln furnace," *Journal of the Air & Waste Management Association*, vol. 48, pp. 44-51, 1998.
- [67] R. Remus, M. Aguado Monsonet, S. Roudier, and L. Delgado Sancho, "JRC reference report," *Best Available Techniques (BAT) Reference Document for Iron and Steel Production*, 2013.
- [68] R. K. Zahl, L. A. Haas, and J. Engesser, "Formation of NO_x in iron oxide pelletizing furnaces," University of Minnesota 1995.
- [69] A. Gunnarsson, "Experimental and numerical studies of thermal radiation in gas, coal and co-fired pilot test facilities," Licentiate thesis, Energy and Environment, Chalmers University of Technology, 2017.
- [70] T. N. Zwietering, "The degree of mixing in continuous flow systems," *Chemical Engineering Science*, vol. 11, pp. 1-15, 1959.
- [71] T. Mendiara and P. Glarborg, "Ammonia chemistry in oxy-fuel combustion of methane," *Combustion and Flame*, vol. 156, pp. 1937-1949, 10// 2009.
- [72] L. S. Jensen, "NO_x from cement production-Reduction by Primary Measures," 1999.
- [73] H. Thunman, F. Niklasson, F. Johnsson, and B. Leckner, "Composition of volatile gases and thermochemical properties of wood for modeling of fixed or fluidized beds," *Energy & Fuels*, vol. 15, pp. 1488-1497, 2001.
- [74] R. Edland, F. Normann, C. Fredriksson, and K. Andersson, "Implications of Fuel Choice and Burner Settings for Combustion Efficiency and NO_x Formation in PF-Fired Iron Ore Rotary Kilns," *Energy & Fuels*, vol. 31, pp. 3253-3261, 2017.
- [75] S. Chen, M. Heap, D. Pershing, and G. Martin, "Influence of coal composition on the fate of volatile and char nitrogen during combustion," in *Symposium (International) on Combustion*, 1982, pp. 1271-1280.
- [76] K. Andersson, F. Normann, F. Johnsson, and B. Leckner, "NO Emission during Oxy-Fuel Combustion of Lignite," *Industrial & Engineering Chemistry Research*, vol. 47, pp. 1835-1845, 2008/03/01 2008.